Kinetic Model of a Low-Pressure N_2–O_2 Flowing Glow Discharge

Boris F. Gordiets, Carlos M. Ferreira, Vasco L. Guerra, Jorge M. A. H. Loureiro, Jacimar Nahorny, Daniel Pagnon, Michel Touzeau, and Marinette Vialle

***Abstract*—A self-consistent kinetic model is developed to study dc flowing glow discharges in N_2/O_2 mixtures. This model includes the calculation of electron energy distribution functions and electron rate coefficients coupled with detailed vibrational kinetics of N_2 molecules, chemical kinetics taking into account a large set of neutral, excited and charged species, interaction of N and O atoms at the discharge tube wall, and the thermal balance of the discharge. The results of this model agree reasonably well with the measurements of the electronic density, the gas temperature, the reduced electric field, the vibrational temperature of N_2, and the concentration of O, N atoms, NO molecules, $N_2(C)$, $N_2^+(B)$, and NO(γ) excited states. The comparison was performed in a N_2–O_2 discharge at pressure $p = 2$ Torr, for discharge currents $I = 15$, 30, and 80 mA, a flow rate $Q = 100$ sccm, and O_2 percentages ranging from 0 up to 100%.**

I. Introduction

THE KINETIC processes occurring in low-temperature plasmas of the atmospheric gases N_2, O_2 and their mixtures are presently the subject of many investigations due to their importance in atmospheric and ionospheric physics, and in plasma chemistry in general. In fact, the knowledge of the kinetics of formation of active N and O atoms, N(^{2}D), $O_2(^1\Delta)$, $N_2(A^3\Sigma)$ metastables, and NO molecules is important to understand the workings of plasma reactors used for chemical synthesis, air pollution cleaning, or for surface treatments of various materials.

Recently, various experiments have been performed on microwave and dc discharges in N_2–O_2 at low pressures (up to a few Torr) [1]–[7], and theoretical models have been developed to analyze the kinetic processes in such discharges and to interpret the experimental results [3], [6], [7]. In a recent paper [7], we have reported an investigation on the kinetics of N atoms and NO molecules production in dc N_2–O_2 glow discharges for a pressure of 2 Torr and various discharge currents, as a function of the relative mixture composition. Measurements of N and NO concentrations, reduced electric field E/N_g (N_g denoting the total gas density), electron density n_e, gas temperature T_g, and vibrational temperature T_v of $N_2(X)$ molecules have been reported over the complete range of relative oxygen concentration (0–100%). A kinetic model was also developed in [7] to interpret the experiments. The model included a detailed analysis of the kinetics of vibrational levels and of a large number of neutral and ionic species, as well as of the discharge thermal balance. This model, however, relied upon estimates of electron transport and collisional data in the mixture based on extrapolations of data previously obtained in pure N_2 or O_2.

In the present work, the model presented in [7] is extended and largely improved by the inclusion of self-consistent electron data calculated from the Boltzmann equation for the precise plasma mixture conditions. Further, in order to build a more comprehensive and manageable kinetic model we have eliminated from the previous model all those species whose concentrations are negligibly small under the experimental conditions of interest here. This leads to a considerable reduction in the total number of reactions to be taken into account (more than 400 in [7]) and in computing time. At the same time, a deeper physical insight into the main discharge workings results.

The experimental investigation reported in [7] is also extended here and new results are presented and compared to the model predictions. In particular, measurements of O, $N_2(C)$, NO(γ), and $N_2^+(B)$ are further reported.

The organization of the paper is the following. In Section II, a detailed discussion of the model is presented. Section III describes the experiments; a summary of the apparatus and the techniques used in [7] is given; and the diagnostics used for the new measurements are described in detail. Section IV presents a detailed comparison between model predictions and measurements along with a discussion of the basic kinetic processes occurring in the discharge. Finally, in Section V we present the main conclusions of this work and discuss guidelines for future research.

II. Kinetic Model

A self-consistent, radially homogeneous kinetic model for glow discharges in flowing N_2–O_2 mixtures has been developed which includes the electron Boltzmann equation, the rate balance equations for the most important neutral and ionic species present in the discharge, the equations describing the vibrational kinetics of $N_2(X)$ molecules, and the thermal balance equation for the gas. These equations are strongly coupled and have been solved altogether in a consistent way,

Manuscript received August 31, 1994; revised November 22, 1994. This work was carried out under the scientific cooperation agreement between the "Centre National de la Recherche Scientifique–France" and the "Junta Nacional de Investigação Científica e Tecnológica–Portugal." J. Nahorny was supported by C.N.Pq.–Brazil.

B. F. Gordiets is with the Centro de Electrodinâmica—Instituto Superior Técnico, 1096 Lisboa Codex, Portugal, on leave from the Lebedev Physical Institute, Moscow, Russia.

C. M. Ferreira, V. L. Guerra, and J. M. A. H. Loureiro are with the Centro de Electrodinâmica—Instituto Superior Técnico, 1096 Lisboa Codex, Portugal.

J. Nahorny, D. Pagnon, M. Touzeau, and M. Vialle are with L.P.G.P.—Université Paris-Sud, 91405 Orsay Cedex, France.

IEEE Log Number 9412952.

0093–3813/95$04.00 © 1995 IEEE

as a function of the discharge operating parameters, viz., gas pressure, initial mixture composition, mass flow rate, current density, tube radius, initial gas temperature, and wall temperature.

This model determines, as a function of the axial coordinate z, the radially averaged populations in the vibrational levels $N_2(X^1\Sigma_g^+, v)$ and the excited states $N_2(A^3\Sigma_u^+, B^3\Pi_g, a'^1\Sigma_u^-, a^1\Pi_g, C^3\Pi_u, a''^1\Sigma_g^+)$, $O_2(a^1\Delta_g, b^1\Sigma_g^+)$, $N(^2D, ^2P)$, and $O(^1D, ^1S)$, as well as the concentrations of other neutral species created via dissociation channels or other chemical reactions ($N(^4S)$, $O(^3P)$, O_3, $NO(X^2\Pi_r)$, N_2O), of the electrons and of the main positive and negative ions present in the discharge (N_2^+, N_4^+, O^+, O_2^+, NO^+, O^-). This model further determines the gas temperature T_g and the reduced maintenance electric field E/N_g under steady-state operating conditions.

This theoretical approach is a heavy task that involves large computing time. For this reason, as mentioned above, the kinetics of heavy species have been considerably simplified here as compared to that developed in [7]. This simplification could be made taking into account the calculations in [7]; they have shown that the concentrations of species other than those included here are negligibly small and have no noticeable influence on the discharge kinetics. Nevertheless, it should be noted that the influence of the states $N_2(W^3\Delta_u, B'^3\Sigma_u^-, w^1\Delta_u)$ and $O_2(A^3\Sigma_u^+, C^3\Delta_u, c^1\Sigma_u^-)$ has indirectly been considered. In fact, the excitation of these states by electronic collisions has been taken into account but we have assumed a fast decay from $N_2(W, B')$ to $N_2(B)$ and from $N_2(w)$ to $N_2(a')$ due to the strong radiative and collisional coupling between these groups of states. As to the oxygen states, we have assumed that excitation of $O_2(A, C, c)$ entirely results in dissociation of $O_2 \rightarrow 2O(^3P)$.

A. Boltzmann Equation

The electron energy distribution function is self-consistently determined here by solving the steady-state, homogeneous electron Boltzmann equation using the usual two-term expansion in spherical harmonics. The mathematical techniques used are similar to those previously reported in [8]–[10]. In [9], the case of a mixture of two molecular gases has already been considered.

Due to the large fractional populations in the vibrationally excited levels $N_2(X, v)$, both inelastic and superelastic collisions of electrons with $N_2(X, v > 0)$ states have been taken into account. However, only inelastic collisions from $O_2(X, v = 0)$ and $NO(X, v = 0)$ have been considered due to the negligibly small populations in the vibrationally excited levels of these species. For similar reasons, superelastic collisions of electrons with electronically excited states (N_2^*, O_2^*, N^*, O^*) have been neglected. The following simplifications have further been made in solving the Boltzmann equation: i) the excitation of electronic states was treated as a single energy loss process assuming that all molecules of each species are in the ground level, $v = 0$, of the electronic ground state; ii) ionization by electron impact was treated similarly to an excitation with a single energy loss and the creation of secondary electrons was neglected.

The electron cross sections used in this paper are the same as in previous works in pure N_2 [8] and pure O_2 [10]. Here, however, we have further included the electron cross sections for excitation of the atomic states $N(^2D, ^2P)$ from $N(^4S)$ [11] and for ionization of NO [12]. The excitation of the $N(^2D, ^2P)$ states was already considered in [13]. Other processes induced by electron collisions such as ionization from $N_2(A)$ [14] and dissociative recombination of N_2^+, O_2^+, NO^+, and N_4^+ ions (see Table I, and [15]–[24] therein) have also been included using semi-empirical formulas for the corresponding rate coefficients versus the electron kinetic temperature.

B. Vibrational Kinetics

The Boltzmann equation is coupled through the fractional populations in the $N_2(X, v)$ levels to the system of master equations for these populations. This system accounts for the following processes as previously described in [3] and [7]:

—Vibrational–excitation and de-excitation by electron impact (e-V)

$$e + N_2(v) \rightleftharpoons e + N_2(w). \tag{1}$$

—Vibration–vibration (V-V) energy exchanges

$$N_2(v+1) + N_2(w) \rightleftharpoons N_2(v) + N_2(w+1) \tag{2}$$
$$N_2(v+1) + O_2(0) \rightleftharpoons N_2(v) + O_2(1) \tag{3}$$
$$N_2(v+1) + NO(0) \rightleftharpoons N_2(v) + NO(1). \tag{4}$$

—Vibration–translation (V-T) energy exchanges

$$N_2(v) + M \rightleftharpoons N_2(v-1) + M \tag{5}$$

with $M = N_2, O_2, N, O, NO$.

—De-excitation in collisions with the wall

$$N_2(v) + \text{wall} \rightarrow N_2(v-1) + \text{wall}. \tag{6}$$

—Chemical reactions leading to the formation or the destruction of NO

$$N_2(v) + O \rightarrow N + NO \tag{7}$$
$$N + NO \rightarrow N_2(\bar{v} = 3.4) + O. \tag{8}$$

—Vibrational excitation due to the quenching of excited $O(^1D)$ atoms

$$O(^1D) + N_2 \rightarrow O(^3P) + N_2(\bar{v} = 2.2). \tag{9}$$

Following [25], we have assumed that the cross sections $\sigma(v \rightleftharpoons v+n)$ for the e-V processes (1) between excited vibrational levels are given by the expression

$$\sigma(v \rightleftharpoons v+n) = \sigma(0 \rightleftharpoons n)(1 + 0.05v)^{-1}. \tag{10}$$

Values up to $n = 10$ were considered but electron excitation of all vibrational levels above $v = 20$ were discarded.

TABLE I
RATE CONSTANTS OF DISSOCIATIVE RECOMBINATION OF IONS N_2^+, O_2^+, NO^+, AND N_4^+ AND BRANCHING RATIO OF DISSOCIATIVE PRODUCTS

Ion	rate constant (cm3/s)	products	branching ratio	ref.
N_2^+	$1.8 \times 10^{-7}(300/T_e)^{0.39}$	$N(^4S)$	1	[15]
		$N(^2D)$	0.9	[16]
		$N(^3P)$	< 0.1	[17]
O_2^+	$2.7 \times 10^{-7}(300/T_e)^{0.7}$	$O(^3P)$	1.15	[15,18]
	$(T < 1200K)$	$O(^1D)$	0.85	[19,20]
	$1.6 \times 10^{-7}(300/T_e)^{0.55}$	$O(^1S)$	< 0.1	[21]
	$(T > 1200K)$			
NO^+	$4.2 \times 10^{-7}(300/T_e)^{0.85}$	$N(^4S)$	0.2	[18,22]
		$N(^2D)$	0.8	[23]
N_4^+	$2.3 \times 10^{-6}(300/T_e)^{0.53}$	-	-	[24]

The rate coefficients for the V-V energy exchanges have been calculated using the following equation [26], [27]:

$$Q_{v+1,v}^{w,w+1} = Q^{01}\delta_v\delta_w F_{vw}(1.5 - 0.5 \times F_{vw}) \tag{11}$$

with F_{vw}, δ_v, and δ_w given by

$$F_{vw} = \exp\{-\delta_{VV}^0 \times (E_{v+1} - E_v - E_{w+1} + E_w)/(2\Delta E)\} \tag{12}$$

$$\delta_v = (v+1) \times (1 + v\Delta E/E_1) \tag{13}$$

and

$$\delta_w = (w+1) \times (1 + w\Delta E/E_1). \tag{14}$$

The parameters Q^{01} and δ_{VV}^0 are given by the following formulas in the case of N_2–N_2 collisions [28]

$$Q^{01}(\mathrm{cm}^3 \cdot \mathrm{s}^{-1}) = 2.5 \times 10^{-14}(T_g/300)^{1.5} \tag{15}$$

$$\delta_{VV}^0 = 6.8/T_g^{\,0.5} \tag{16}$$

with T_g in *Kelvin*.

For N_2–O_2 collisions we have similarly used

$$Q^{01}(\mathrm{cm}^3 \cdot \mathrm{s}^{-1}) = 1.7 \times 10^{-13}(T_g/300)^{1.5} \tag{17}$$

$$\delta_{VV}^0 = 6.92/T_g^{\,0.5} \tag{18}$$

while for N_2–NO collisions we used

$$Q^{01}(\mathrm{cm}^3 \cdot \mathrm{s}^{-1}) = 1.3 \times 10^{-14}(T_g/300)^{1.5} \tag{19}$$

$$\delta_{VV}^0 = 7.02/T_g^{\,0.5}. \tag{20}$$

In (12)–(14) ΔE and E_1 are connected with the anharmonic *Morse* oscillator parameters through the expressions $\Delta E = \hbar\omega\chi_e$ and $E_1 = \hbar\omega(1 - 2\chi_e)$, with

$$E_v = \hbar\omega[(v + 0.5) - \chi_e(v + 0.5)^2].$$

Only the levels $v = 0$ and $v = 1$ of O_2 and NO are accounted for in the model because the higher vibrational levels of both molecules are efficiently destroyed by fast V-T exchanges with O atoms. It is still interesting to note that resonances occur between the first vibrational levels of O_2 and NO and the levels $N_2(v = 28, 27)$ and $N_2(v = 15, 14)$, respectively.

The rate coefficients for the V-T processes take the form [27]

$$P_{v,v-1}^{(M)} = P_{10}^{(M)}\,\delta_v \exp(\delta_{VT}^{(M)} v) \tag{21}$$

where $P_{10}^{(M)}$ and $\delta_{VT}^{(M)}$ depend on the type of the colliding particle M (M = N_2, O_2, N, O, NO). In the case of the molecular species N_2, O_2, and NO, we have taken $\delta_{VT}^{(M)}$ equal to the parameters for V-V collisions given by (16), (18), and (20), respectively. The parameter $P_{10}^{(M)}$ has been assumed the same for the colliding particles N_2, O_2, NO and equal to the semi-empirical value obtained for V-T (N_2–N_2) collisions [29]. This approximation is well justified since the dominant V-T processes occur through N_2–O collisions. On the other hand, since vibrationally excited $O_2(X, v)$ and NO(X, v) molecules are present in small amounts, the V-V reactions between N_2–O_2 and N_2–NO correspond, in fact, to depopulating mechanisms for $N_2(X, v)$ (with larger rate coefficients than those for V-T processes). Finally, for V-T energy exchanges in N_2–O collisions we have used an analytical approximation to fit the experimental data for $P_{10}^{(0)}$ [30], [31]. We have taken $\delta_{VT}^{(0)} = 0$ due to the lack of data for transitions involving upper levels.

We have not included in our model V-T exchanges in N_2–N collisions because available calculations of rate coefficients for these processes [32], [33] result in too fast a relaxation of the vibrationally excited molecules $N_2(X, v \geq 15)$. This in turn results in too small populations in these levels and in strong gas heating which has not been experimentally confirmed in pure N_2 discharges.

Reaction (7) is a very important channel for the production of NO. This reaction was first investigated in the context of upper atmosphere chemistry [34]. Its rate coefficient is probably strongly dependent on the vth level of N_2. However, no experimental data are available and the existing theoretical calculations are in disagreement by two orders of magnitude [35]–[37]. Here, we assume the rate coefficient for this reaction to be given by a simple step function of the vth level as follows:

$$K_7(\mathrm{cm}^3 \cdot \mathrm{s}^{-1}) = \begin{cases} 1.3 \times 10^{-10} \exp(-E_a/T_g), & \text{if } E_v < E_a \\ 10^{-11}, & \text{if } E_v \geq E_a \end{cases} \tag{22}$$

where E_a = 38 000 K is the activation barrier. The value of K_7 for $E_v \geq E_a$ (hereafter referred to as K_7^0) is the largest one reported in the literature and it seems to be justified by the comparison between theory and experiment presented below (see Section IV).

The excitation of the $N_2(v = 1-12)$ levels is also possible via the exothermic reaction (8), which is the reverse of reaction (7). The percentage energy transferred to the vibrational mode in reaction (8) is about 25% [38], which corresponds on the average to the excitation of 3.4 vibrational quanta of N_2. Due to the lack of information about the exact dependence of this rate on the vth level, we have assumed the value given in Table VI and considered that 3.4 vibrational quanta are excited on the average per reaction.

TABLE II
RATE CONSTANTS OF QUENCHING AND EXCITATION OF N_2 ELECTRONIC LEVELS BY COLLISIONS WITH ATOMS AND MOLECULES

R-	process	k(cm³/s)	ref.
R1	$N_2(A) + O(^3P) \rightarrow NO + N(^2D)$	7×10^{-12}	[39-41]
R2	$\rightarrow N_2(X) + O(^1S)$	2.1×10^{-11}	[39-41]
R3	$N_2(A) + N(^4S) \rightarrow N_2(X) + N(^4S)$	2×10^{-12}	[42]
R4	$\rightarrow N_2(X) + N(^2P)$	$4 \times 10^{-11}(300/T)^{2/3}$	[43-45]
R5	$N_2(A) + O_2(X) \rightarrow N_2(X) + O_2(B)$	$2.1 \times 10^{-12}(T/300)^{0.55}$	[46-49]
R6	$\rightarrow N_2(X) + O_2(a)$	$2 \times 10^{-13}(T/300)^{0.55}$	[47-49]
R7	$\rightarrow N_2(X) + O_2(b)$	$2 \times 10^{-13}(T/300)^{0.55}$	[47-49]
R8	$\rightarrow N_2O + O(^3P)$	$2 \times 10^{-14}(T/300)^{0.55}$	[47-49]
R9	$N_2(A) + N_2(X) \rightarrow 2N_2(X)$	3×10^{-16}	[50]
R10	$N_2(A) + N_2(X, v > 30) \rightarrow N_4^+ + e$	10^{-13}	this work
R11	$N_2(A) + NO \rightarrow N_2(X) + NO(A)$	6.9×10^{-11}	[51]
R12	$N_2(A) + N_2O \rightarrow N_2(X) + N(^4S) + NO$	10^{-11}	[59,62]
R13	$N_2(A) + N_2(A) \rightarrow N_2(X) + N_2(B)$	3×10^{-10}	[53,54]
R14	$\rightarrow N_2(X) + N_2(C)$	1.5×10^{-10}	[55]
R15	$N_2(A) + N_2(X, v > 5) \rightarrow N_2(B) + N_2(X, v-6)$	10^{-10}	[56,57]
R16	$N_2(B) + N_2(X, v-6) \rightarrow N_2(A) + N_2(X, v > 5)$	10^{-10}	this work
R17	$2N_2(X, v > 11) \rightarrow N_2(X) + N_2(A)$	10^{-16}	[56]
R18	$N_2(B) + O_2(X) \rightarrow N_2(X) + O + O$	3×10^{-10}	[56-62]
R19	$N_2(B) + NO \rightarrow N_2(A) + NO$	2.4×10^{-10}	[59]
R20	$2N_2(X, v > 13) \rightarrow N_2(X) + N_2(B)$	10^{-15}	[55]
R21	$N_2(C) + N_2(X) \rightarrow N_2(a') + N_2(X)$	10^{-11}	[46,61]
R22	$N_2(C) + O_2(X) \rightarrow N_2(X) + O + O$	3×10^{-10}	[56,62]
R23	$N_2(a') + N_2(X) \rightarrow N_2(B) + N_2(X)$	1.9×10^{-13}	[58,63]
R24	$N_2(a') + O_2(X) \rightarrow N_2(X) + O + O$	2.8×10^{-11}	[62,63]
R25	$N_2(a') + NO \rightarrow N_2(X) + N + O$	3.6×10^{-11}	[62,63]
R26	$N_2(a') + N_2(A) \rightarrow N_4^+ + e$	1.5×10^{-11}	this work
R27	$2N_2(a') \rightarrow N_4^+ + e$	10^{-11}	this work

R-	process	k(cm³/s)	ref.
R28	$N_2(v > 16) + N_2(v > 16) \rightarrow N_2(a') + N_2(X)$	10^{-15}	this work
R29	$N_2(a'') + N_2(X) \rightarrow N_2(X) + N_2(X)$	10^{-14}	[65]
R30	$N_2(a'') + N_2(X, v > 12) \rightarrow N_4^+ + e$	$10^{-11} exp(-640/T)$	this work
R31	$2N_2(X, v > 24) \rightarrow N_2(X) + N_2(a'')$	1.6×10^{-15}	[66]
	three-body collisions	k (cm⁶/s)	ref.
R32	$N + N + M \rightarrow N_2(A) + M$	$1.7 \times 10^{-33}(M = N_2, O_2, NO)$ $10^{-32}(M = N, O)$	[67,68,71]
R33	$N + N + M \rightarrow N_2(B) + M$	$2.4 \times 10^{-33}(M = N_2, O_2, NO)$ $1.4 \times 10^{-32}(M = N, O)$	[68-71]

Finally, the excitation of the vth levels of N_2 is also possible through the quenching of the excited atomic state $O(^1D)$ (reaction (9)). We have used for this reaction a similar procedure as for reaction (8), with a rate coefficient as given in Table V.

C. Kinetics of Electronically Excited Molecules and Other Chemical Reactions

In addition to all electron impact and vibrational kinetic processes referred to above our model further includes a large number of physical–chemical reactions, which determine the populations of the electronically excited molecular/atomic states $N_2(A,\ B,\ a',\ a,\ C, a'')$, $O_2(a, b)$, $N(^2D, ^2P)$, and $O(^1D, ^1S)$, as well as the concentrations of the species N, O, NO, N_2O, and O_3, and of the positive and negative ions N_2^+, N_4^+, O^+, O_2^+, NO^+, and O^-.

A complete list of the processes considered is given in the Tables II–X, along with the corresponding rate coefficients selected from the literature ([39]–[118]). Some processes involving collisions of electronically excited heavy particles are not simple de-excitation reactions since in many cases such collisions result in chemical reactions. In particular, the

TABLE III
RATE CONSTANTS OF QUENCHING AND EXCITATION OF O_2 ELECTRONIC LEVELS BY COLLISIONS WITH ATOMS AND MOLECULES

-	process	k(cm³/s)	ref.
R34	$O_2(a) + O(^3P) \rightarrow O_2(X) + O$	7×10^{-16}	[62,72]
R35	$O_2(a) + N(^4S) \rightarrow NO + O$	$2 \times 10^{-14} exp(-600/T)$	[62]
R36	$O_2(a) + O_2(X) \rightarrow O_2(X) + O_2(X)$	$3.8 \times 10^{-18} exp(-205/T)$	[74]
R37	$O_2(a) + N_2(X) \rightarrow O_2(X) + N_2(X)$	3×10^{-21}	[62]
R38	$O_2(a) + NO \rightarrow O_2(X) + NO$	2.5×10^{-11}	[76]
R39	$O_2(a) + O_3 \rightarrow 2O_2(X) + O(^1D)$	$5.2 \times 10^{-11} exp(-2840/T)$	[77,78]
R40	$O_2(a) + O_2(a) \rightarrow O_2(X) + O_2(b)$	$7 \times 10^{-28} T^{3.8} exp(700/T)$	[79]
R41	$O(^3P) + O_3 \rightarrow O_2(X) + O_2(a)$	$10^{-11} exp(-2300/T)$	[77,78]
R42	$O_2(b) + O(^3P) \rightarrow O_2(a) + O(^3P)$	8.1×10^{-14}	[62,80]
R43	$O_2(b) + O_2(X) \rightarrow O_2(a) + O_2(X)$	$4.3 \times 10^{-22} T^{2.4} exp(-281/T)$	[81]
R44	$O_2(b) + N_2(X) \rightarrow O_2(a) + N_2(X)$	$1.7 \times 10^{-15}(T/300)$	[82]
R45	$O_2(b) + NO \rightarrow O_2(a) + NO$	6×10^{-14}	[83,84]
R46	$O_2(b) + O_3 \rightarrow 2O_2 + O$	2.2×10^{-11}	[77,80,82]
	three-body collisions	k (cm⁶/sec)	ref.
R47	$O + O + M \rightarrow O_2$(all states) + M	$k_{com} = 10^{-32} T^{-0.63} (M = O_2)$ $3.6 k_{com}$ (M=O) $0.25 k_{com}$ (M=N_2,N)	[71]
R48	$\rightarrow O_2(a) + M$	$0.07 k_{com}$ (M)	[85]
R49	$\rightarrow O_2(b) + M$	$< 0.01 k_{com}$ (M)	[86]
R50	$O_2(a) + O_2(a) + O_2(X) \rightarrow 2O_3$	10^{-31}	[77]

TABLE IV
RATE CONSTANTS OF QUENCHING OF METASTABLE LEVELS OF NITROGEN ATOMS BY COLLISIONS WITH ATOMS AND MOLECULES

-	process	k(cm³/s)	ref.
R51	$N(^2D) + O(^3P) \rightarrow N(^4S) + O(^1D)$	4×10^{-13}	[16,87]
R52	$N(^2D) + O_2 \rightarrow NO + O$	5.2×10^{-12}	[88]
R53	$N(^2D) + N_2 \rightarrow N(^4S) + N_2$	6×10^{-15}	[62,59]
R54	$N(^2D) + NO \rightarrow N_2 + O$	1.8×10^{-10}	[59,89]
R55	$N(^2D) + N_2O \rightarrow NO + N_2$	3.5×10^{-12}	[59,90]
R56	$N(^2P) + N(^4S) \rightarrow N + N$	1.8×10^{-12}	[56]
R57	$N(^2P) + O(^3P) \rightarrow N + O$	10^{-12}	present work
R58	$N(^2P) + O_2(X) \rightarrow NO + O$	2.6×10^{-15}	[91]
R59	$N(^2P) + N_2(X) \rightarrow N(^4S) + N_2(X)$	2×10^{-18}	[89]
R60	$N(^2P) + NO \rightarrow N_2 + O$	3×10^{-11}	[62]

TABLE V
RATE CONSTANTS OF QUENCHING OF METASTABLE LEVELS OF NITROGEN ATOMS BY COLLISIONS WITH ATOMS AND MOLECULES

-	process	k(cm³/s)	ref.
R61	$O(^1D) + O(^3P) \rightarrow O(^3P) + O(^3P)$	8×10^{-12}	[92]
R62	$O(^1D) + O_2(X) \rightarrow O(^3P) + O_2(a)$	10^{-12}	[92]
R63	$\rightarrow O(^3P) + O_2(b)$	$2.6 \times 10^{-11} exp(67/T)$	[62,86,92]
R64	$O(^1D) + N_2(X) \rightarrow O(^3P) + N_2(X)$	2.3×10^{-11}	[97]
R65	$O(^1D) + O_3 \rightarrow O_2 + 2O(^3P)$	2.3×10^{-10}	[92,93]
R66	$O(^1S) + O(^3P) \rightarrow O(^1D) + O(^1D)$	$5 \times 10^{-11} exp(-301/T)$	[62,94]
R67	$O(^1S) + N(^4S) \rightarrow O(^3P) + N$	10^{-12}	[95]
R68	$O(^1S) + O_2(X) \rightarrow O(^3P) + O_2$	$4 \times 10^{-12} exp(-865/T)$	[96]
R69	$O(^1S) + N_2(X) \rightarrow O(^3P) + N_2(X)$	10^{-17}	[97]
R70	$O(^1S) + O_2(a) \rightarrow O(^3P) + O_2(C + A)$	1.1×10^{-10}	[98,99]
R71	$\rightarrow O(^1D) + O_2(b)$	2.9×10^{-11}	[98,99]
R72	$\rightarrow 3O(^3P)$	3.2×10^{-11}	[98,99]
R73	$O(^1S) + NO \rightarrow O(^3P) + NO$	8×10^{-10}	[100,101]
R74	$O(^1S) + O_3 \rightarrow 2O_2(X)$	6×10^{-10}	[100]

TABLE VI
RATE CONSTANTS OF BIMOLECULAR NITROGEN–OXYGEN REACTIONS

-	process	k(cm³/s)	T (K)	ref.
R75	$N + NO \rightarrow O + N_2$	$1.8 \times 10^{-11}(T/300)$	200-4000	[62,71,102]
R76	$N + O_2 \rightarrow O + NO$	$3.2 \times 10^{-12}(T/300)exp(-3150/T)$	300-3000	[62,71,103]
R77	$N + O_3 \rightarrow NO + O_2$	$< 2 \times 10^{-16}$	300	[62,71,104]
R78	$O + O_3 \rightarrow O_2 + O_2$	$2 \times 10^{-11}exp(-2280/T)$	220-1000	[62,71,105]
	associative ionization			
R79	$2N_2(v > 32) \rightarrow N_4^+ + e$	$3.5 \times 10^{-15}exp(-1160/T)$	300	[66]

TABLE VII
RATE CONSTANTS OF ATOM RECOMBINATION WITH CREATION OF MOLECULES N_2, O_2, NO, O_3, N_2O

-	process	k(cm⁶/s)	T (K)	ref.
R80	$N + N + M \rightarrow N_2 + M$	$8.3 \times 10^{-34}exp(500/T)(M = N_2)$	100-600	[62,71,103]
		$1.9 \times 10^{-33}(M = N)$	600-6300	[62,71,103]
		$k_{O_2} = k_{NO} = k_{N_2}$		
		$k_O = k_N = 6k_{N_2}$		
R81	$O + O + M \rightarrow O_2 + M$	$2.7 \times 10^{-34}exp(720/T)(M = N_2)$	200-500	[71,105]
		$6.2 \times 10^{-32}T^{-0.63}(M = N)$	500-4000	[62,71,105]
		$2.5 \times 10^{-31}T^{-0.63}(M = O)$	300-4000	[71,105]
		$k_N = k_{NO} = 0.25k_{O_2}$		
		$k_O = 3.6k_{O_2}$		
R82	$N + O + M \rightarrow NO + M$	$1.03 \times 10^{-32}(300/T)^{0.5}$ for any M	200-2000	[62,71,103]
R83	$O + O_2 + M \rightarrow O_3 + M$	$6.2 \times 10^{-34}(300/T)^2(M = N)$	220-1000	[62,71,105]
		$6.9 \times 10^{-34}(300/T)^{1.25}(M = O_2)$	220-1000	[62,71,105]
		$2.1^{-34}exp(245/T)(M = O)$		[71]
R84	$N_2 + O + M \rightarrow N_2O + M$	see [71]	220-1000	[71]

processes involving vibrationally excited molecules $N_2(X, v)$ play an important role in the whole kinetics. The collision of two molecules $N_2(X, v)$ in high vibrational levels can result in excitation of the states $N_2(A)$, $N_2(B)$, $N_2(a')$, $N_2(a'')$ (see reactions R17, R20, R28, R31), or in associative ionization (reaction R79). Collisions between vibrationally excited and electronically excited N_2 molecules can also re-excite the molecule into another state (reactions R15, R16) or result in associative ionization (reactions R10, R30). Associative ionization can further result from collisions between electronically excited molecules (reactions R26, R27).

Unfortunately, the rate coefficients for some processes are poorly known, the available data being often scattered over two orders of magnitude (e.g., the rate coefficient of reaction (7) for formation of NO).

As a consequence of the complex kinetics involved here, a number of species are formed with high translational energy and may not be in thermal equilibrium with the background gas. This is, for example, the case of N atoms created by collisions of O atoms with vibrationally excited $N_2(X, v)$ molecules in levels $v \geq 13$ (reaction (7)). These hot N atoms can in turn react with O_2 yielding O and NO according to reaction R76 in Table VI [119]. However, the rate coefficient for these reactions with hot atoms should be considerably larger than the equilibrium rate given in Table VI. For this reason, we have estimated the concentration of hot N atoms and the correction to the equilibrium rate constant for reaction R76 using the same procedures as in [7].

TABLE VIII
RATE CONSTANTS FOR REACTIONS INVOLVING POSITIVE IONS

-	process	k(cm³/s)	ref.
R85	$O^+ + N_2 \rightarrow NO^+ + N$	$(1.53 - 1.97 \times 10^{-3}T + 9.56 \times 10^{-7}T^2) \times 10^{-12}$	[106,107]
R86	$O^+ + O_2 \rightarrow O_2^+ + O$	$2 \times 10^{-11}(300/T)^{0.5}$	[108]
R87	$O^+ + O_3 \rightarrow O_2^+ + O_2$	10^{-10}	[108]
R88	$O^+ + NO \rightarrow NO^+ + O$	2.4×10^{-11}	[109]
R89	$O^+ + N_2O \rightarrow NO^+ + NO$	2.3×10^{-10}	[109]
R90	$\rightarrow N_2O^+ + O$	2.2×10^{-10}	[109]
R91	$\rightarrow O_2^+ + N_2$	2×10^{-11}	[110]
R92	$N_2^+ + O_2 \rightarrow O_2^+ + N_2$	$6 \times 10^{-11}(300/T)^{0.5}$	[56,111]
R93	$N_2^+ + O \rightarrow NO^+ + N(^4S,^2D)$	$1.3 \times 10^{-10}(300/T)^{0.5}$	[112]
R94	$\rightarrow O^+ + N_2$	$10^{-11}(300/T)^{0.5}$	[112]
R95	$N_2^+ + O_3 \rightarrow O_2^+ + O + N_2$	10^{-10}	[62]
R96	$N_2^+ + N \rightarrow N^+ + N_2$	$7.2 \times 10^{-13}(T/300)$	[56]
R97	$N_2^+ + NO \rightarrow NO^+ + N_2$	3.3×10^{-10}	[112]
R98	$N_2^+ + N_2O \rightarrow N_2O^+ + N_2$	5×10^{-10}	[110]
R99	$\rightarrow NO^+ + N + N_2$	4×10^{-10}	[110]
R100	$O_2^+ + N_2 \rightarrow NO^+ + NO$	10^{-17}	[111]
R101	$O_2^+ + N \rightarrow NO^+ + O$	1.2×10^{-10}	[112]
R102	$O_2^+ + NO \rightarrow NO^+ + O_2$	6.3×10^{-10}	[117]
R103	$N_4^+ + N_2 \rightarrow N_2^+ + 2N_2$	$2.1 \times 10^{-16}exp(T/121)$	[56]
R104	$N_4^+ + O_2 \rightarrow O_2^+ + 2N_2$	2.5×10^{-10}	[114]
R105	$N_4^+ + O \rightarrow O^+ + 2N_2$	2.5×10^{-10}	[62]
R106	$N_4^+ + NO \rightarrow NO^+ + 2N_2$	4×10^{-10}	[62]
	three-body collisions	k (cm⁶/s)	ref.
R107	$N_2^+ + N_2 + N_2 \rightarrow N_4^+ + N_2$	5×10^{-29}	[112]
R108	$O^+ + N_2 + M \rightarrow NO^+ + N + M$	$6^{-29}(300/T)(M = N_2, O_2)$	[112]

-	process	k(cm³/s)	ref.
R109	$O^+ + O + M \rightarrow O_2^+ + M$	$10^{-29}(M = N_2, O_2)$	[62]
R110	$O^+ + N + M \rightarrow NO^+ + M$	$10^{-29}(M = N_2, O_2)$	[62]

TABLE IX
RATE CONSTANTS FOR REACTIONS INVOLVING NEGATIVE O^- IONS

-	electron detachment	k(cm³/s)	ref.
R111	$O^- + O \rightarrow O_2 + e$	1.4×10^{-10}	[77]
R112	$O^- + N \rightarrow NO + e$	2.6×10^{-10}	[110]
R113	$O^- + O_2 \rightarrow O_3 + e$	5×10^{-15}	[62,116]
R114	$O^- + O_2(a) \rightarrow O_3 + e$	3×10^{-10}	[77]
R115	$O^- + O_2(b) \rightarrow O + O_2 + e$	6.9×10^{-10}	[117]
R116	$O^- + N_2(A) \rightarrow O + N_2 + e$	2.2×10^{-9}	[117]
R117	$O^- + N_2(B) \rightarrow O + N_2 + e$	1.9×10^{-9}	[118]

D. Interactions with the Wall

Although the model developed in this work does not account for the variations in the species concentrations with radius (we recall that the model is radially homogeneous), the losses resulting from diffusion to the wall followed by deactivation at the wall need to be considered for various species. We assume that the corresponding radially averaged rates for wall loss ν can be expressed as

$$\nu = \left(\frac{\Lambda^2}{D} + \frac{2R}{\gamma\langle v\rangle}\right)^{-1}. \qquad (23)$$

TABLE X
RATE CONSTANTS OF PROCESSES INVOLVING POSITIVE AND NEGATIVE IONS

-	two-body collisions	reactants	k(cm³/s)	ref.
R118	$O^- + B^+ \to O + B$	$B^+ = O^+, O_2^+, N^+, N_2^+, NO^+$	$2\times10^{-7}(300/T)$	[62,115]
R119	$O^- + BC^+ \to O + B + C$	$BC^+ = O_2^+, N_2^+, N_4^+, NO^+$	10^{-7}	[62,115]
	three-body collisions	reactants	k (cm⁶/s)	ref.
R120	$O^- + B^+ + M \to O + B + M$	$B^+ = O^+, O_2^+, N^+, N_2^+, NO^+$ $M = N_2, O_2$	$2\times10^{-25}(300/T)^{2.5}$	[62,115]
R121	$O^- + B^+ + M \to O + B + M$	$B^+ = O^+, O_2^+, N^+$ $M = N_2, O_2$	$2\times10^{-25}(300/T)^{2.5}$	[62,115]

Here, D denotes the diffusion coefficient, Λ is the characteristic diffusion length, R is the tube radius, $\langle v\rangle$ is the average velocity of the particles, and γ is the wall deactivation probability (fraction of wall collisions leading to destruction of the species). As expected on physical grounds, (23) shows that if the deactivation probability is low, then the average rate constant for wall loss depends primarily on this probability and the tube diameter. On the other hand, if this probability is high, then the loss rate may primarily be controlled by the rate of diffusion to the wall.

Besides the recombination of the positive ions with electrons and the destruction of metastable species at the walls, atomic reassociation of N and O atoms and vibrational de-excitation of $N_2(v)$ molecules at the wall were considered. Specifically, we have taken into account the following heterogeneous processes, with the corresponding probabilities given in brackets:

$$N_2(v) \to N_2(v-1),\ (\gamma = 7\times10^{-3})\ [13] \quad (24)$$
$$N_2(A) \to N_2(X),\ (\gamma = 1) \quad (25)$$
$$N_2(a') \to N_2(B),\ (\gamma = 1) \quad (26)$$
$$O_2(a) \to O_2(X),\ (\gamma = 2\times10^{-5}) \quad (27)$$
$$O_2(b) \to O_2(X),\ (\gamma = 2\times10^{-2}) \quad (28)$$
$$N(^2D) \to N(^4S),\ (\gamma = 1) \quad (29)$$
$$N(^2P) \to N(^4S),\ (\gamma = 1) \quad (30)$$
$$O(^1D) \to O(^3P),\ (\gamma = 1) \quad (31)$$
$$O(^1S) \to O(^3P),\ (\gamma = 1). \quad (32)$$

Further, wall losses of $O(^3P)$ and $N(^4S)$ atoms are important loss channels for these species. However, the corresponding probabilities are only approximately known for discharges in the pure gases, no data being available for mixtures. It is however known that the probability for wall reassociation of $O(^3P)$ atoms decreases when N_2 is added to pure O_2 [4]. For lack of data, we have worked out a simple kinetic model to account for wall losses of O and N atoms assuming that such losses result from a reaction of a gas phase atom impinging on the wall or of physisorbed atoms with chemisorbed atoms. This model accounts for the reactions resulting in adsorption of O and N atoms at vacant sites on the wall and for the heterogeneous reactions of gas phase O and N atoms with O_s and N_s (the subscript s holding for adsorbed atoms) leading to the formation of gas phase O_2, N_2, and NO molecules. Since the rate constants for these reactions and their temperature dependence are unknown, we have estimated these data from a best fit of the calculated to the measured concentrations of O and NO throughout the whole range of experimental conditions considered in this work. Measurements of the N atom concentration in the case of pure N_2 and of N_2 with a small admixture of O_2 (not reported in this paper) were also used for the above estimates. Additional measurements of N covering the whole range of mixture compositions are now underway in order to improve the accuracy of this kinetic model for wall losses. Details about this are beyond the scope of the present paper and will be presented elsewhere (however, see further Section IV).

The rate of loss of the positive ions by diffusion to the wall and subsequent recombination with electrons was also treated here in an approximate manner since an exact formulation taking into account the presence of all types of positive ions and of O^- would constitute a formidable task. In fact, this problem is not simple to solve even when just only one type of positive ion and one type of negative ion are simultaneously present [120].

The calculations of our model have shown that the concentration of O^- is always smaller (or even much smaller at low to moderate O_2 relative concentrations) than that of the electrons, except for very high O_2 percentages and low currents, in which case both concentrations become comparable. In the former case, since negative ions are only present in relatively small amounts the rate of escape of the positive ions to the wall is governed by the classical ambipolar diffusion coefficient. In the latter case, our model calculations show that the detachment rate is always much larger than the mean ionization rate per electron under the present conditions; therefore, the ratio of the negative ion density to the electron density is expected to be nearly constant across most of the tube radius and to fall down abruptly only in a thin boundary layer close to the tube wall [120]. This being so, in spite of the strong electronegativity of the plasma the rate of escape of positive ions to the wall is also practically the same as if negative ions were absent, that is, this rate is again governed by the classical ambipolar diffusion coefficient (this conclusion can easily be inferred from the results reported in [120] for the above conditions, even though it was not explicitly stated in that paper).

For the above reasons, we have assumed that for all mixture compositions the rate for wall loss of positive ions is simply given by D_a/Λ^2, where $D_a \simeq \mu_i u_k$ is the classical ambipolar diffusion coefficient, μ_i and u_k denoting the ion mobility and the electron characteristic energy, respectively. The values of μ_i have been taken from [121] while those of u_k were calculated from the solutions to the electron Boltzmann equation.

Finally, note that O^- is not lost to the wall since negative ions are fully confined in the plasma volume by the space-charge field [120].

E. Thermal Balance

A self-consistent calculation of the gas temperature T_g is also included in the present model since the vibrational distribution function of $N_2(X)$ molecules and some reaction rate coefficients are strongly dependent on T_g. For this purpose, the thermal balance for the gas has been considered. The main sources of gas heating are the V-T and V-V vibrational relaxation mechanisms of $N_2(X)$ molecules, the deactivation of electronically excited states of N_2, O_2, N, O in collisions with heavy particles, the exothermic chemical reactions either between neutrals, or ions, or ions and neutrals, and electronic collisions. The latter include the elastic collisions, the collisions leading to rotational excitation of N_2 and O_2, to vibrational excitation of O_2, and to dissociation of both N_2 and O_2 (which produce hot dissociated atoms), by electron impact and, finally, dissociative electron attachment to O_2 molecules. On the other hand, thermal conduction to the tube wall is the main gas cooling mechanism.

We have assumed a parabolic radial gas temperature profile, in agreement with experimental evidence [122] and as a first approximation we neglected the radial dependence of the coefficient of thermal conductivity for the gas mixture λ arising from its dependence on T_g. In this case, it can readily be shown that the power density loss by thermal conduction is given by $8\lambda(T_g - T_w)/R^2$, where T_g is the radially averaged gas temperature and T_w is the wall temperature. The gas temperature on the axis of the tube is equal in this case to $(2T_g - T_w)$. The values of T_w have been taken from experiment, while those of λ have been estimated from data for pure N_2 and O_2 using simple transport theory for binary mixtures.

F. Gas-Flow Model and Solution Algorithm

Since all the experiments were conducted in the presence of a small gas flow it is necessary to account for the gas dynamics effects in the model. This was done using a very simple approach. Assuming that the pressure is approximately constant along the tube axis, z, the conservation of the mass flow rate implies that the average gas velocity $v(z)$ must vary along z proportionally to T_g, that is

$$v(z) = v(z=0)T_g(z)/T_g(z=0)$$

where $z = 0$ corresponds to the point where the fresh gas enters the positive column. The value of $v(z=0)$ is simply calculated from the experimental mass flow rate, which is an input parameter of the model. Diffusion of the species and thermal conduction along the tube have not been considered, therefore, we assume that the variation along z of all calculated quantities X_i is simply obtained from the expression

$$dX_i/dz = v^{-1}(z) \times dX_i/dt.$$

The time evolution of the species concentrations is of course governed by the corresponding kinetic master equations starting from an unexcited N_2–O_2 mixture at time $t = 0$.

Fig. 1 gives a flow chart of the complete model which illustrates both the coupling between the various modules and the solution algorithm used. The calculations are performed for given values of pressure p, fractional mixture composition

$$\delta = \frac{[O_2]}{[N_2] + [O_2]}$$

tube radius R, discharge current I, gas flow rate Q, and axial distribution of the wall temperature, $T_w(z)$. The calculated results include the reduced maintenance field E/N_g, the concentrations of heavy neutral species (including the manifold of $N_2(X, v)$ levels) and ions N_j, the electron concentration n_e, the mean gas temperature T_g, and the vibrational temperature of $N_2(X, v)$ molecules T_v. The latter is defined here as the temperature of the Boltzmann distribution that best fits the populations of the lowest four vibrational levels of $N_2(X)$. These calculated data are obtained iteratively according to the scheme shown in Fig. 1. The calculation starts assuming initial values for these data. A first iterative loop consists in solving the Boltzmann equation (BE) for this set of initial values (taking into account the effects of inelastic and superelastic collisions with vibrationally excited $N_2(X)$ molecules), and, then, calculating the pertinent electron transport and collisional data, and the discharge current. The ratio E/N_g is changed until the calculated current equals the fixed value. The electron rate coefficients so obtained are then used in the master equations for all the neutral and ionic species and in the thermal balance equation, which are solved to yield new values for N_j, T_g, T_v, N_g, and n_e, the latter being obtained from the difference between the concentrations of the positive and the negative ions. These new values so obtained are then taken as initial values and the iterations proceed until either the prefixed residence time or a steady-state situation is reached. In both cases, the number of iterations is automatically adjusted

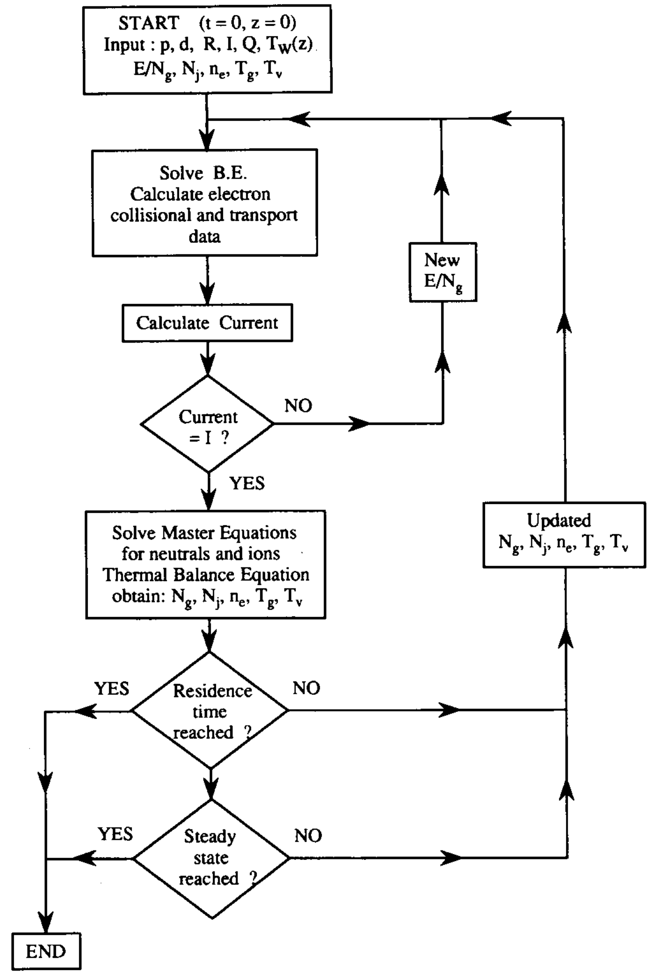

Fig. 1. Flow chart of the model.

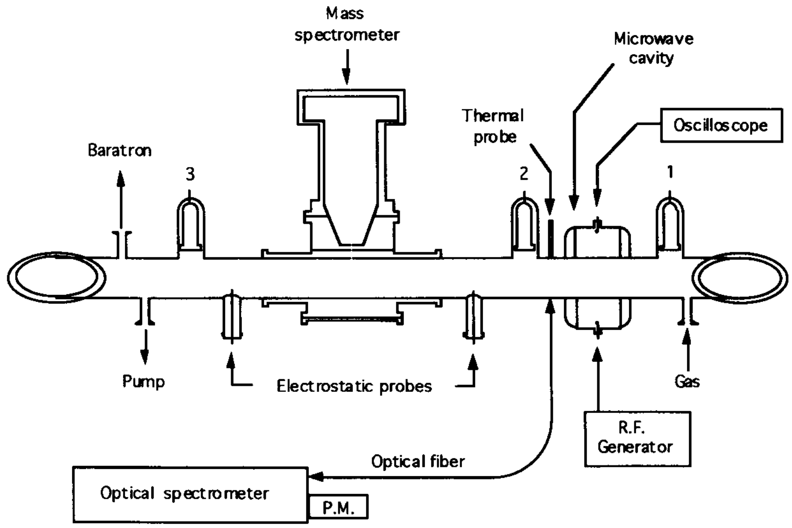

Fig. 2. Schematic diagram of the apparatus used for mass spectrometry and optical emission diagnostics.

by the subroutine in order to insure that convergence is sufficiently accurate.

The measurements reported in this paper were performed far downstream the discharge entrance, at positions where the steady state has already been attained. All the calculations were therefore performed for such conditions.

III. Experimental

The experimental study of the discharge is performed by using two identical devices. The first apparatus is devoted to the measurements of the NO concentration by mass spectrometry and to the optical diagnostics by emission spectroscopy. The relative concentration of the nitrogen atoms in the discharge and in the afterglow is measured by two-photon laser-induced fluorescence (LIF) using another device.

A schematic diagram of the first apparatus is represented in Fig. 2. A dc glow discharge is created between two electrodes in a 16-mm-diameter Pyrex tube. Two configurations are studied. The discharge is created between electrodes 1 and 3 in order to measure the concentration of NO molecules in the discharge. When the discharge is established between electrodes 1 and 2, the concentrations of NO molecules and the optical emission are measured in the flowing afterglow. The pressure is regulated by a butterfly throttling valve monitored by a capacitance MKS gauge. The relative composition of the mixture, δ, is determined by the ratio of N_2 and O_2 measured mass flow rates. Typical experimental conditions are: pressure: $p = 2.0$ Torr; discharge current: $I = 5$–80 mA; total mass flow rate: $Q = 100$ sccm; $\delta = 0$–100%; mean gas velocity at the discharge entrance: $v \simeq 4$ ms^{-1}.

The electron density n_e is determined from the shift of the resonance frequency of a microwave cavity tuned on the TM_{010} mode. The electron density increases from $\simeq 5 \times 10^9$ cm^{-3} up to $\simeq 2 \times 10^{10}$ cm^{-3} when the discharge current is varied from 15 to 80 mA and decreases slowly when the O_2 percentage increases [7].

The maintenance electric field E of the discharge is measured by the difference in potential between two identical electrostatic probes.

The gas temperature is determined by measuring the rotational distribution of the $N_2(C^3\Pi_u - B^3\Pi_g)$ 337-nm emission band for $0 < \delta < 95\%$ and of the atmospheric $O_2(b^1\Sigma - X^3\Sigma)$ 760-nm band in the predominant oxygen mixture ($90 < \delta < 100\%$) [7], [122] with a high-resolution monochromator (Jobin-Yvon THR).

The pressure is measured with a Baratron capacitance manometer. In our conditions, i.e., a flow of 100 sccm, 2.0 Torr in a 16-mm inner diameter tube the pressure is constant along the tube. The total concentration N_g and the reduced electric field E/N_g are then calculated using the ideal gas law $p = N_g k T_g$.

The N_2 vibrational distribution calculated in Section II is characterized by the vibrational temperature T_v of the lowest vibrational levels $v \leq 4$. T_v is deduced from the vibrational distribution of the $N_2(C^3\Pi_u, v')$ excited states, determined by measuring the emission of the vibrational sequence $\Delta v = v' - v''$ of the second positive system $N_2(C, v') \rightarrow N_2(B, v'')$. The determination of T_v is detailed in [7]. Typical values are: $T_v = (3000 \pm 500)$ K for $I = 15$ mA, $T_v = (4000 \pm 500)$ K for $I = 30$ mA, $T_v = (5500 \pm 500)$ K for $I = 80$ mA. No significant variation of T_v versus O_2 percentages is observed in the range where this diagnostic is reliable.

The concentration of NO molecules is determined in the discharge and in the afterglow by a mass spectrometer (VG SPX300) coupled to the Pyrex tube by a differential pumping system. The calibration of the mass spectrometer is performed by injecting a controlled NO mass flow rate into the N_2–O_2 flow when the discharge is off.

The concentration of nitrogen atoms in the discharge and in the afterglow is measured by detecting the emission of the $N(^4D^0) \rightarrow N(^4P^0)$ 869-nm fluorescence induced by a two-photon laser transition at 211 nm. The experimental setup is shown in Fig. 3. A laser energy of ~ 1 mJ per pulse at 211 nm with a 7-ns pulse time duration and 10-Hz repetition rate is generated by a pulsed tunable Quantel Datachrom 5000 system. The laser beam is focused with a 35-cm focal length lens into a 16-mm diameter Pyrex tube in which two holes of 2.2-mm diameter allow the laser to cross the

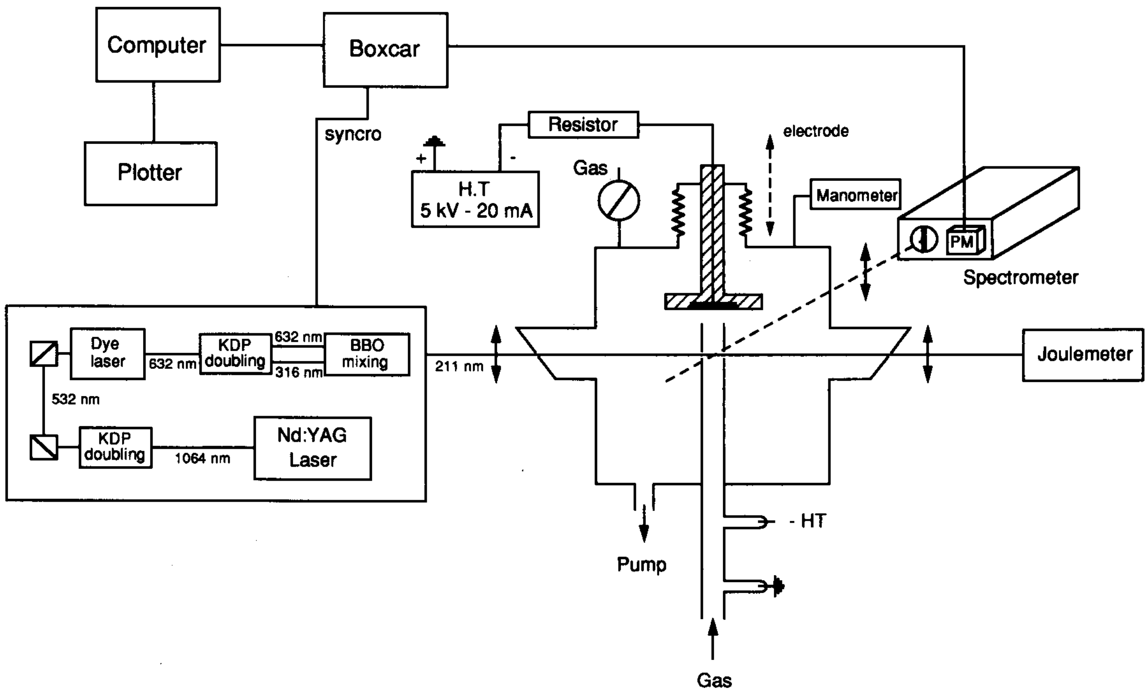

Fig. 3. Schematic diagram of the apparatus used to measure the nitrogen atom concentration by a two-photon laser-induced fluorescence technique (LIF).

positive column or the flowing afterglow of the discharge. The fluorescence is detected perpendicularly to the laser beam with a monochromator (Jobin-Yvon H640), a photomultiplier, and a 4420 EG & G boxcar averager. A more detailed discussion of this technique is presented in [123]. The calibration of the LIF measurements in the discharge is made from absolute N atoms concentrations measurements performed by NO titration as described in [7].

The emission of the second positive system $N_2(C-B)$, first negative system $N_2^+(B-X)$, NO (γ) bands and of the oxygen atom lines as well as the emission of argon lines when a small percentage of argon is introduced into the discharge are measured with a monochromator (Jobin-Yvon HR320) and a multichannel analyzer.

The concentration of oxygen atoms is determined by actinometry using argon as actinometer. This technique has already been used to investigate pure O_2 discharges and its validity has been studied by comparing actinometric measurements to VUV absorption measurements in the same experimental conditions [124]. Measurements are performed using the experimental setup represented in Fig. 2. A constant mass flow rate $q = 1$ sccm of argon is introduced in the N_2–O_2 mixture. The oxygen transition O $(3p^3P \rightarrow 3s^3S)$ 844.6 nm and the argon transition $Ar(2p^9 \rightarrow 1s^5)$ 811.5 nm have been selected because they are sufficiently strong even for small δ values and they are not perturbed by the emission of the first positive system of N_2 which is weak for wavelengths above 800 nm. To determine the concentration [O] of the oxygen atoms in the ground state we have assumed the following kinetics for the creation and loss of the excited states of oxygen and argon. The Ar $(2p_9)$ excited state is principally populated by direct excitation by electron impact

$$e + \mathrm{Ar}\,(1p_0) \overset{k_{2p_9}}{\rightarrow} e + \mathrm{Ar}\,(2p_9) \tag{33}$$

and lost by radiative de-excitation or quenching by oxygen or nitrogen molecules

$$\mathrm{Ar}\,(2p_9) \overset{A_{2p_9}}{\rightarrow} \mathrm{Ar}\,(1s^5) + h\nu \text{ (811.5 nm)}$$
$$\mathrm{Ar}\,(2p_9) + M \overset{k_M^{2p_9}}{\rightarrow} \mathrm{Ar} + M \tag{34}$$

where $M = N_2, O_2$, $A_{2p_9} = 3.66 \times 10^7\ s^{-1}$ is the emission probability [125], $k_M^{2p_9}$ is the quenching coefficient for the 811.5-nm line by M species. As these quenching coefficients are unknown, we have assumed a value

$$k_{O_2}^{2p_9} = k_{N_2}^{2p_9} = 0.44 \times 10^{-9} \mathrm{cm}^3 \cdot \mathrm{s}^{-1}$$

which corresponds to a mean value of the coefficients for quenching of the 750.4- and 751.5-nm argon lines by oxygen, measured by Belikov [126]. The excitation coefficient k_{2p_9} is calculated from the following relation:

$$k_{2p_9} = \sqrt{\frac{2e}{m}} \int_{u_s}^{\infty} \sigma(u) f(u) u \, du \tag{35}$$

where $\sigma(u)$ is the excitation cross section for the Ar $(2p_9)$ state, u_s the threshold energy for the reaction, $f(u)$ is the electron energy distribution function (eedf), and m and e are the electron mass and absolute charge, respectively. The values of k_{2p_9} have been calculated using the cross section of [127] and the eedf determined in Section II for $0 \leq \delta \leq 1$ and three values of the discharge current, $I = 15, 30, 80$ mA. In steady state, the concentration of Ar $(2p_9)$ excited state is given by the relation

$$\mathrm{Ar}\,(2p_9) = \frac{k_{2p_9} n_e\,[\mathrm{Ar}]}{A_{2p_9} + k_M^{2p_9}([\mathrm{N}_2] + [\mathrm{O}_2])}. \tag{36}$$

O $(3p^3P)$ is excited by electronic impact with the atomic ground state

$$e + \mathrm{O}\,(2p^4.{}^3P) \overset{k^{3P}}{\rightarrow} e + \mathrm{O}\,(3p^3P) \tag{37}$$

or by dissociative excitation of oxygen molecules by electronic impact

$$e + \mathrm{O}_2 \overset{k_{\mathrm{diss}}}{\rightarrow} e + \mathrm{O}\,(3p^3P) + \mathrm{O}. \tag{38}$$

The main loss processes for the $\mathrm{O}\,(3p^3P)$ state are the radiative transition

$$\mathrm{O}\,(3p^3P) \overset{A_{3P}}{\rightarrow} \mathrm{O}\,(3s^3S) + h\nu\ (844.6\ \mathrm{nm}) \tag{39}$$

and quenching by oxygen or nitrogen molecules

$$M + \mathrm{O}\,(3p^3P) \overset{k_M^{3P}}{\rightarrow} M + \mathrm{O}. \tag{40}$$

We have taken the value $A_{3P} = 2.8\times10^7\ \mathrm{s}^{-1}$ [125]. A mean value $k_{\mathrm{O}_2}^{3P} = 7.5 \times 10^{-10}\ \mathrm{cm}^3\cdot\ \mathrm{s}^{-1}$ is taken for the quenching coefficient by oxygen molecules according to [128]–[130] and a mean value $k_{\mathrm{N}_2}^{3P} = 4.2 \times 10^{-10}\ \mathrm{cm}^3\cdot\ \mathrm{s}^{-1}$ is taken for the quenching coefficient by nitrogen molecules [128]–[131].

The coefficients k_{3P} and k_{diss} are calculated from (35) using cross sections from [128], [132], [133] for the excitation of $\mathrm{O}\,(3p^3P)$ and from [134] for dissociative excitation, for $0 \le \delta < 1$ and $I = 15, 30, 80$ mA. It can be shown that for all values of δ, k_{diss} is always three orders of magnitude smaller than k_{3P}. The contribution of dissociative excitation is then neglected. In steady state, the concentration of $\mathrm{O}\,(3p^3P)$ excited state is given by the relation

$$[\mathrm{O}\,(3p^3P)] = \frac{k_{3P} n_e [\mathrm{O}\,(2p_4\cdot{}^3P)]}{A_{3P} + k_{\mathrm{O}_2}^{3P}[\mathrm{O}_2] + k_{\mathrm{N}_2}^{3P}[\mathrm{N}_2]}. \tag{41}$$

The oxygen- and argon-line intensities are proportional to the concentration of the excited states

$$\begin{aligned} I(844) &= A_{3P}[\mathrm{O}\,(3p^3P)]h\nu_{844} \\ I(811) &= A_{2p_9}[\mathrm{Ar}\,(2p_9)]h\nu_{811}. \end{aligned} \tag{42}$$

Taking into account (36) and (41) and the values of the spectral transfer function $\Re_{844}$ and $\Re_{811}$ of the detection device at 844 and 811 nm, respectively, we can deduce the concentration of ground-state oxygen atoms from the measurement of the ratio $(I_{844}/_{811})_{\mathrm{mes}}$ using the relation

$$\begin{aligned} \frac{[\mathrm{O}]}{N_g} &= \frac{[\mathrm{Ar}]}{N_g}\left(\frac{I_{844}}{I_{811}}\right)_{\mathrm{mes}} \frac{\Re_{844}}{\Re_{811}} \frac{A_{2p_9}}{A_{3P}} \frac{h\nu_{811}}{h\nu_{844}} \frac{k_{2p_9}}{k_{3P}} \\ &\times \frac{A_{3P} + k_{\mathrm{O}_2}^{3P}[\mathrm{O}_2] + k_{\mathrm{N}_2}^{3P}[\mathrm{N}_2]}{A_{2p_9} + k_{2p_9}([\mathrm{O}_2] + [\mathrm{N}_2])} \end{aligned} \tag{43}$$

where

$$\frac{[\mathrm{Ar}]}{N_g} = \frac{q}{Q} = \frac{1}{100}.$$

Furthermore, to improve the accuracy of these measurements, the values of the concentration of O atoms derived from (43) have been compared to the absolute concentration measured by VUV absorption spectrometry in a pure O_2 discharge [124]. The values deduced by actinometry are multiplied by a correction factor calculated in order to fit to VUV determination for $\delta = 1$ and $I = 80$ mA .

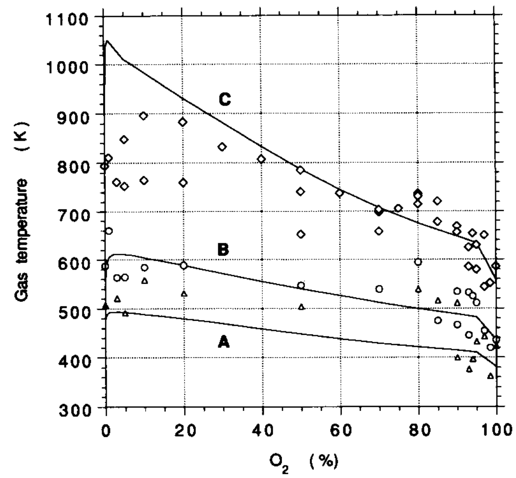

Fig. 4. Variation of gas temperature versus the O_2 percentage for $I = 15$, 30, and 80 mA. The measurements are represented by symbols; triangles: 15 mA; circles: 30 mA; and diamonds: 80 mA. The calculated values are represented by solid lines. *A*: 15 mA; *B*: 30 mA; *C*: 80 mA.

IV. Results and Discussion

Due to the great number of active species interacting in N_2–O_2 dc glow discharges as described in previous sections, the comparison between the model predictions and experimental results needs simultaneous measurements of the concentrations of a great number of species. The different techniques developed to determine the main species concentrations have been described in Section III. For the discharge conditions $p = 2$ Torr, $Q = 100$ sccm, $\delta = 0 - 1, I =$ 15,30, 80 mA, the following plasma parameters have been measured: electron density n_e, gas temperature T_g, reduced electric field E/N_g, vibrational temperature of N_2 molecules T_v, concentration of oxygen and nitrogen atoms, and NO molecules $\mathrm{N}_2(C^3\Pi_u)$, $\mathrm{NO}\,(A^3\Sigma^+)$, and $\mathrm{N}_2^+(B^2\Sigma_u^+)$ excited states.

A comparison between measured and calculated gas temperatures in the central region of the tube is given in Fig. 4. It is seen that reasonable agreement is obtained. The main gas heating mechanism was found to be the exothermic reaction (8). This reaction together with the reverse reaction (7) constitute a very efficient multiquanta de-excitation V-T process for the high N_2 vibrational levels.

As it will be shown in the following, the population of vibrationally excited molecules $\mathrm{N}_2(X, v > 12)$ is strongly destroyed by O atoms. Nevertheless, the characteristic vibrational temperature for the lowest vibrational levels remains approximately constant for $\delta =$ 0–0.9. The calculations of the model yield the values $T_v = 3200$, 4200, and 6000 K for $I = 15$, 30, and 80 mA, respectively. These values are in reasonable agreement with those experimentally determined by a spectroscopic technique [7].

As shown in Fig. 5, reasonable agreement is also obtained between the experimental and calculated variation of the electron density versus the O_2 percentage. The calculated electron density is however overestimated by about 40% at the higher current.

Further comparisons between calculations and experiment are discussed below.

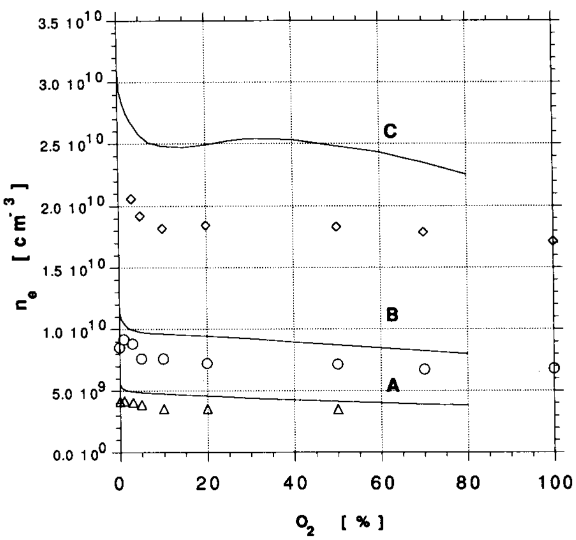

Fig. 5. Variation of electron density versus the O_2 percentage. The calculated values are represented by solid lines. The symbols are as in caption to Fig. 4.

A. NO Molecules

The results of measurements and calculations of the concentration of NO molecules are reported in Fig. 6(a) and (b). For all δ values, the main source of NO molecules is reaction (7)

$$N_2(v > 12) + O \rightarrow NO + N.$$

All calculations, including results of Fig. 6(a) and (b) have been performed with the value $k_7^0 = 10^{-11}$ cm^3· s^{-1}, in agreement with the theoretical calculations [37], which gives an interpretation of the $N_2^+(B \rightarrow X)$ emission as discussed in Section IV-F. We have verified that the calculated NO concentration is not strongly changed if the magnitude of the rate constant k_7^0 for this reaction is varied in the range 10^{-13}–10^{-11} cm^3· s^{-1} [7]. In our experimental conditions, reaction (7) is the main process for relaxation of N_2 vibrational levels $N_2(v \geq 12)$. A change in k_7^0 induces only a change in the populations of $N_2(v \geq 12)$ vibrational levels but does not change the molecular flux $k_7^0[O]\Sigma_{v \geq 12}[N_2(v)]$ which is the main channel for production of NO and N. This process is very efficient and leads to such large concentrations of [NO] and [N] that reaction (8) becomes the main channel for losses of NO and N. The rate of production of [NO] [N] by reaction (7) is approximately equal to the rate of destruction of [NO] [N] by reaction (8). So the concentration of NO molecules and N atoms, if considered separately, are dependent on other processes of production and loss such as the production of NO molecules by the reaction

$$N + O_2 \rightarrow O + NO$$

(R76) and loss of N atoms at the wall.

The role of this process can be amplified because "hot" N atoms with energy greater than the energy threshold 0.27 eV can be produced by reaction (7). The importance of this effect is discussed in [7]. It has been shown that this process should be taken into account for $\delta > 0.1$ if a value of $k_7^0 = 10^{-13}$ cm^3· s^{-1} is adopted. However, with the value of $k_7^0 = 10^{-11}$ cm^3· s^{-1} taken in this work the calculations are not very sensitive to the production of "hot" N atoms.

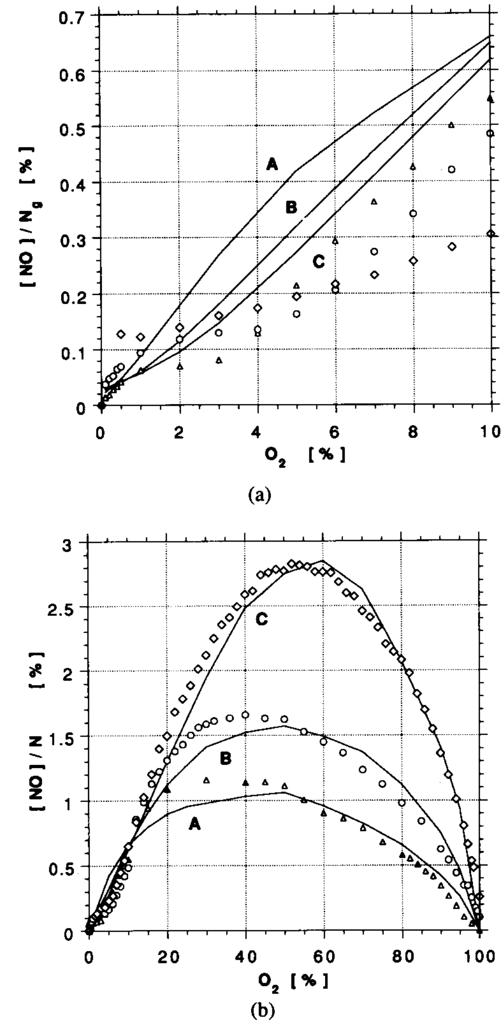

Fig. 6. Variation of the NO concentration inpercentage of the gas concentration N_g versus the O_2 percentage of the N_2/O_2 mixture in the positive column of a N_2/O_2 flowing glow discharge (Pressure p = 2 Torr, mass flowrate $[N_2] + [O_2]$= 100 sccm). (a) A blow up for O_2 percentage ranging from 0 to 10% of (b) for 15, 30, and 80 mA. The symbols are as in caption to Fig. 4.

The probability γ_N of N atom losses on a Pyrex wall in N_2–O_2 discharges is presently unknown. In [7] it was shown that a constant γ_N value of 10^{-4} leads to calculated NO concentrations lower than the experimental ones for $\delta \geq 0.6$ even if the other parameters for production and losses of NO molecules are varied. Here, however, we have assumed that wall losses of N atoms lead to the formation of NO instead of N_2. As discussed in Section II-D, a simple kinetic model for surface reactions of N and O atoms has been developed which shows that the probability γ_N depends then on the ratio X =[O]/[N] and the gas temperature. The independent parameters of this kinetic model have been adjusted here from the best fit of the calculated values of [NO] to the experimental ones (note that the calculations of [NO] are sensitive to γ_N). For example, according to this model, when δ is varied from 0.1 to 0.95, X increases from 10 up to 10^4 and γ_N increases from 6×10^{-4} to 2×10^{-2}, for a current of 80 mA.

The NO concentrations calculated with these assumptions are reported in Fig. 6(a) and (b). There is good agreement with experiment in the whole range of δ values, especially for $\delta \geq 0.6$ where a poor agreement was obtained using a

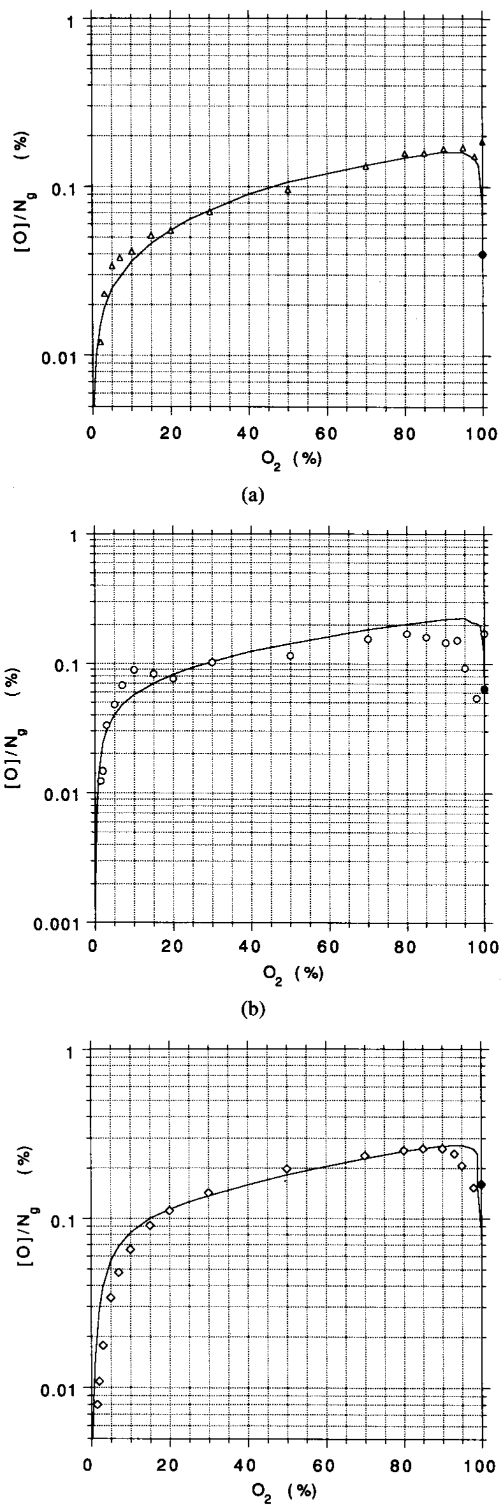

Fig. 7. Variation of the oxygen atom concentration in percentage of the gas concentration N_g versus the O_2 percentage in a N_2/O_2 positive column determined by actinometry (see Section III). The open symbols are as in the caption to Fig. 4. The full symbols are the values determined in a pure O_2 discharge by VUV absorption spectroscopy. The value at 80 mA is taken to calibrate the actinometric determinations. (a) 15 mA; (b) 30 mA; (c) 80 mA.

constant $\gamma_N \simeq 10^{-4}$. The production rate of NO and N from reaction (7) is a decreasing function of δ for $\delta \geq 0.2$ due to the decrease in vibrational energy flux towards high vibrational levels, $N_2(v \geq 12)$. This is caused by the decrease in N_2 concentration and also by the increase in V-T relaxation as δ increases. Nevertheless, an increase in NO concentration is observed when δ is varied from 0 to 0.5 because the losses of N atoms by reaction (R76) and wall reactions increase. A decrease in NO concentration is only observed for $\delta \geq 0.5$.

B. Oxygen Atoms

The calculated values of O concentrations are presented on Fig. 7(a)–(c), and compared to the experimental ones measured by actinometry for $0 < \delta \leq 1$ and the discharge currents $I = 15$ mA (Fig. 7(a)), 30 mA (Fig. 7(b)), and 80 mA (Fig. 7(c)). In our experimental conditions, the rate of production and loss of O atoms by direct and reverse reactions (7) and (8) are nearly equal. Oxygen atoms are mainly produced by direct electronic impact dissociation of O_2 molecules and also for $\delta \leq 0.5$ by dissociative collisions of O_2 with $N_2(B)$ and $N_2(a')$ molecules (reactions R18 and R24 in Table II). Processes R52, R54, and R60 involving $N(^2D)$ and $N(^2P)$ metastable atoms can also be important for O production, for δ values smaller than 0.3 and large populations of $N(^2D)$ and $N(^2P)$ metastable atoms. Oxygen atoms are principally lost by reassociation at the discharge tube wall. The reassociation probability γ_O for O atoms in a N_2–O_2 discharge is not known. It is clear from [4] that γ_O rapidly decreases when a small percentage of nitrogen (up to 5%) is added in an oxygen discharge. Such a variation in γ_O explains the increase in O concentration observed in Fig. 7(a)–(c), when δ is varied from 1 to 0.95–0.90. The γ_O value used in the calculations has been determined by fitting the calculated O concentrations to the experimental ones and using the above mentioned model for surface reactions. γ_O is varied versus the ratio $X = [O]/[N]$ and the gas temperature T_g between $\gamma_O = 4 \times 10^{-4}$ up to 2.5×10^{-3}. Even with an adjusted value of γ_O some discrepancies between calculated and experimental [O] concentrations remain for small δ values. This can be explained by the important role of the dissociation processes R18, R24, and R25 by $N_2(B)$ and $N_2(a')$ whose rate coefficients are not reliably known and by existing uncertainties in the kinetics of these states. The kinetic model can explain the important increase in the dissociation degree when a small amount of N_2 is added in pure O_2. This is due to an increase of γ_O caused by a decrease in X.

C. Reduced Electric Field E/N_g

The measured and calculated values of the reduced electric field are compared in Fig. 8(a)–(c). The reduced field exhibits a maximum for O_2 percentages in the range 0.05–0.07. This behavior is related to the importance of associative ionization for very low O_2 percentages. For example, the calculations show that, for $\delta = 10^{-3}$, the associative ionization rate is 80, 40, 15% of the ionization rate by electron impact for discharges currents $I = 80$, 30, 15 mA, respectively. The contribution of associative ionization rapidly decreases when the O_2 percentage increases, since the involved excited states ($N_2(X, v \geq 12), N_2(a')$) are then destroyed by O_2, O, and NO. As a result, the reduced electric field must increase in order to sustain the discharge. The best agreement with experiment

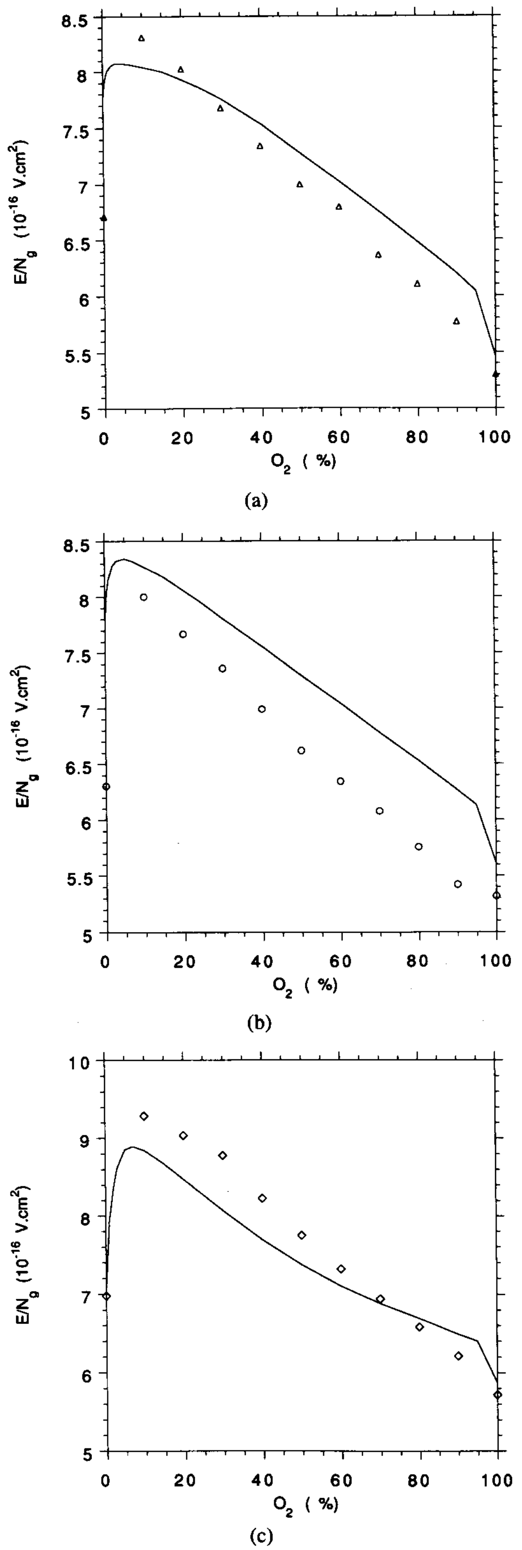

Fig. 8. Variation of the reduced electric field of the positive column versus the O_2 percentage. (a) 15 mA; (b) 30 mA; (c) 80 mA.

is obtained with the following associative ionization rate constants, in $cm^3 \cdot s^{-1}$: $k_{R10} = 10^{-13}$; $k_{R26} = 1.5 \times 10^{-11}$; $k_{R27} = 10^{-11}$; and $k_{R30} = 10^{-11} \times e^{-640/T_g}$ (note, however, that some disagreement remains at the lower currents). These are the values used in Fig. 8(a)–(c) even though they differ by a factor of 2 to 5 from those found in the literature [56], [64], [135].

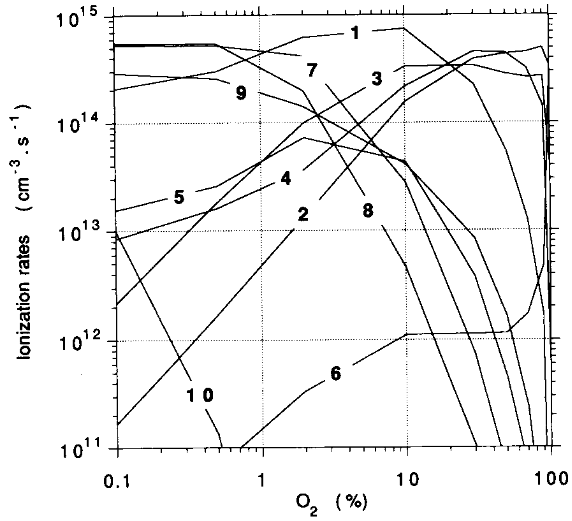

Fig. 9. Variation of the calculated ionization rate constants versus the O_2 percentage for a discharge current $I = 80$ mA, for the following processes: 1, 2, 3, 4: direct ionization of N_2, O_2, O, and NO, respectively; 5, 6: electronic ionization of the $N_2(A)$ and $O_2(a)$ metastable molecules, respectively; 7, 8: associative ionization by reaction between metastable molecules $N_2(A) + N_2(a')$ and $N_2(a') + N_2(a')$, respectively; 9, 10: associative ionization by reaction between $N_2(a'') + N_2(v > 12)$ and $N_2(A) + N_2(v > 30)$, respectively.

As an example, the calculated rates of ionization through different channels are shown in Fig. 9, for a discharge current of 80 mA.

For larger O_2 percentages ($\delta > 0.05$–0.1), associative ionization becomes negligible and the decrease in E/N_g can be explained by the increasing contribution of electron ionization of O, O_2, and NO which have lower ionization thresholds than N_2. For example, for $0.3 < \delta < 0.7$, the relative contribution of O, O_2, and NO to the total ionization rate reaches values of 50, 40, and 30%, for the discharge currents $I = 80$, 30, and 15 mA, respectively. In the same conditions, the contribution of NO is 30, 20, and 15% even if the concentration of NO is low (cf. Fig. 6).

D. Population of $N_2(C)$ State

The intensity of the $N_2(C - B)$ 337-nm band and the excitation rate of the $N_2(C)$ electronic state are compared in Fig. 10. For the purposes of comparison, the calculated and the measured populations have been normalized to the same value for $I = 30$ mA and $\delta = 0.5$. The main process for excitation of $N_2(C)$ is electron impact excitation from ground state $N_2(X)$ molecules while the main loss channel is radiative decay in all our experimental conditions. It can be seen in Fig. 10 that the measured and the calculated $N_2(C)$ populations exhibit the same behavior for O_2 percentages higher than 0.1. The decrease of $N_2(C)$ population when δ increases is the result of the decrease in the rate coefficient for electronic excitation which is due to the decrease both in E/N_g and in $N_2(X)$ concentration. The discrepancy between theory and experiment for O_2 percentages lower than 0.05 and small currents is related to the difference between calculated and measured values of E/N_g for these experimental conditions (see Section IV-C), since the electron rate coefficient for excitation of $N_2(C)$ is very sensitive to changes in E/N_g.

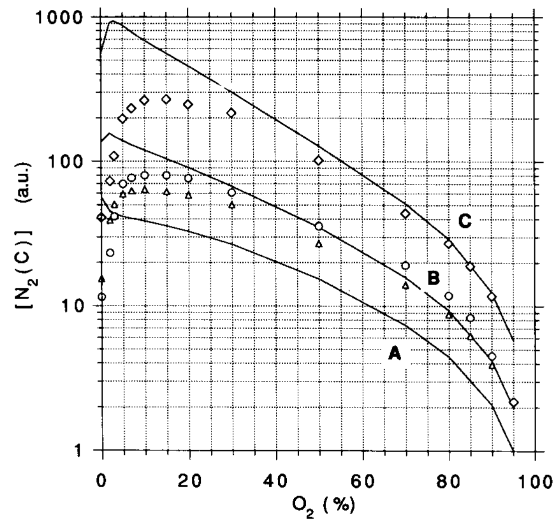

Fig. 10. Variation of the population of the $N_2(C)$ state (in arbitrary units) determined from the emission of the second positive system band $N_2(C-B)$ at 337 nm versus the O_2 percentage for discharge current $I = 15$, 30, and 80 mA. The calculated and the experimental values are adjusted for $I = 30$ mA and O_2 percentage = 50%. The symbols are as in the caption to Fig. 4.

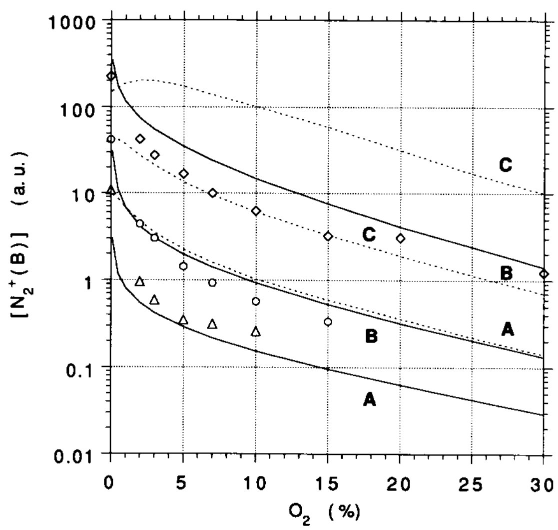

Fig. 12. Variation of the population of $N_2^+(B)$ level (in arbitrary units) determined from the emission of the first negative system at 391 nm versus the O_2 percentage for $I = 15$, 30, and 80 mA. The experimental and the theoretical values are adjusted for pure N_2 and $I = 30$ mA. The solid lines represent the values calculated with a rate constant $k_7^0 = 10^{-11}$ $cm^3 \cdot s^{-1}$ and dashed lines with $k_7^0 = 10^{-13}$ $cm^3 \cdot s^{-1}$.

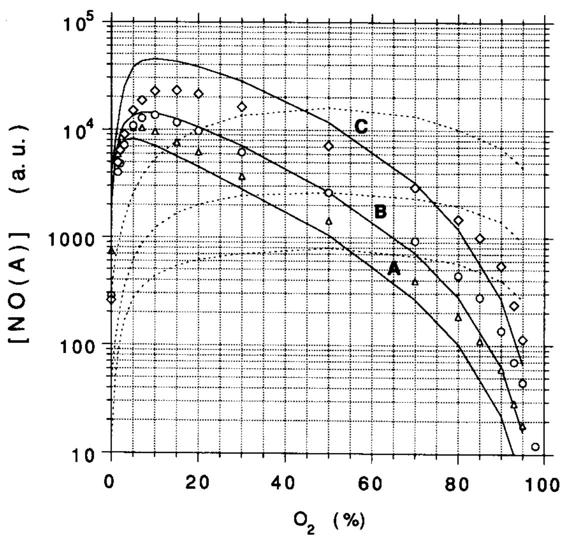

Fig. 11. Variation of the population of $NO(A)$ excited state (in arbitrary units) determined from the emission of the NO_γ at 237 nm versus the O_2 percentage for $I = 15$, 30, and 80 mA. The full lines represent the calculation of the excitation rate of $NO(A)$ by the reaction $N_2(A) + NO(X) \rightarrow NO(A) + N_2$ and the dashed lines by the direct electronic excitation: $e + NO \rightarrow NO(A) + e$. The calculated and experimental values are adjusted for a O_2 percentage of 50% and a discharge current $I =$ 30 mA. Symbols as in caption to Fig. 4.

E. Population of NO (A) Excited State

The measurements and the calculations of the relative intensity of the $NO(\gamma)(NO(A \rightarrow X))$ band at 237 nm are presented in Fig. 11. Again, the experimental and the calculated relative concentrations were normalized to the same value for $I = 30$ mA and $\delta = 0.5$. In order to explain the maximum of intensity measured for O_2 percentages in the range 0.05–0.15, we have investigated two different processes for excitation of $NO(A)$ electronic level:

i) electron excitation of ground state NO molecules

$$e + NO(X) \rightarrow NO(A) + e. \tag{44}$$

ii) E-E energy exchange due to collisions with $N_2(A)$ metastables

$$N_2(A) + NO(X) \rightarrow N_2(X) + NO(A). \tag{45}$$

From the comparison of the rates of production of $NO(A)$ by the above processes to the intensity of the $NO(\gamma)$ band versus O_2 percentages, it can be concluded that the E-E energy exchange is the main process for excitation of $NO(A)$ in our experimental conditions. The increase in the $NO(\gamma)$ band intensity with addition of oxygen for $0 \leq \delta \leq 0.1$ is due to the increase in concentration of NO molecules discussed in Section IV-A (see also Fig. 6) and in the $N_2(A)$ population. The decrease in intensity of the $NO(\gamma)$ band for oxygen percentages above 0.1 is mainly due to the decrease in $N_2(A)$ population, in spite of the growth of [NO] when δ is varied up to 0.5. This decrease in $N_2(A)$ population is due to the decrease of $N_2(X)$ concentration and of E/N_g, and to the increase of quenching by O atoms and NO molecules (which are the main destruction processes of this state in this range of O_2 percentages).

F. Population of $N_2^+(B)$ State

In Fig. 12 are reported the relative intensities of $N_2^+(B \rightarrow X)$ 391.4-nm band versus O_2 percentage. These results are compared to the calculated excitation rate of $N_2^+(B)$ state. The measured intensities show a very fast decrease with addition of O_2 in the discharge. To explain this behavior, three different processes of excitation of the $N_2^+(B)$ state have been investigated. The first one is direct ionization of $N_2(X)$ molecules by electronic impact with creation of $N_2^+(B)$ excited state

$$e + N_2(X) \rightarrow N_2^+(B) + 2e. \tag{46}$$

The second one is excitation of $N_2^+(X)$ ions by electron impact

$$e + N_2^+(X) \rightarrow N_2^+(B) + e. \tag{47}$$

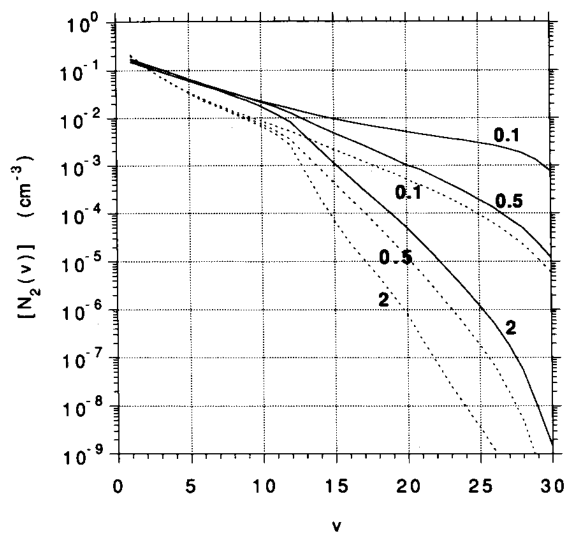

Fig. 13. Vibrational distribution of $N_2(X, v)$ molecules calculated for different O_2 percentages—0.1, 0.5, and 2%. Solid lines correspond to a discharge current $I = 80$ mA and dashed lines to $I = 30$ mA.

The calculated rates of production of $N_2^+(B)$ by these latter processes cannot explain, however, the fast decrease in intensity of the $N_2^+(B)$ 391.4-nm band with increasing δ due to the smooth change of the electron density and the increase of the electron rate coefficients for excitation of $N_2^+(X)$ state as E/N_g increases.

The third excitation process investigated is the exothermic quasiresonant V-E energy exchange in collisions of $N_2^+(X)$ ions with vibrationaly excited N_2 molecules

$$N_2(v > 12) + N_2^+(X) \rightarrow N_2(v - 12) + N_2^+(B). \quad (48)$$

This reaction is an important process for the excitation of $N_2^+(B)$ in pure nitrogen post-discharges [136] and it seems to be the main process for production of $N_2^+(B)$ in our experimental conditions.

The $[N_2^+(X)]\Sigma_{v>12}[N_2(v)]$ flux, which is proportional to the rate of this reaction, has been calculated as a function of δ for the two values $k_7^0 = 10^{-11}$ $cm^3 \cdot s^{-1}$; and $= 10^{-13}$ $cm^3 \cdot s^{-1}$. The results of these calculations reported in Fig. 12 show that the value 10^{-11} $cm^3 \cdot s^{-1}$ leads to better agreement with the observed variation of the $N_2^+(B)$ 391.4-nm band.

Further evidence for the above conclusions is provided in Fig. 13, where the calculated vibrational distribution function of $N_2(X)$ is given for discharge currents of 30 and 80 mA and various percentages of O_2. As the latter increases, reaction (7) causes a strong decrease in the populations of the levels $v > 12$ which can thus explain the fast decay observed in the 1^- system emission.

Moreover, in order that reaction (48) be much faster than reaction (47) the rate constant for the former, k_{48}, can be estimated to be much larger than 10^{-12} $cm^3 \cdot s^{-1}$.

V. Conclusion

We have presented a detailed analysis of kinetic processes in a low-pressure dc N_2–O_2 flowing glow discharge in which the mutual influence of electrons, vibrational and chemical kinetics has been consistently taken into account.

We have shown that the model explains reasonably well a large number of experimental results as a function of the operating conditions, in particular the discharge current and the composition of the N_2–O_2 mixture. The comparison between calculated and experimental data leads to the following main conclusions.

a) The NO, N, and O populations are strongly coupled by the following reactions:

$$N_2(v > 12) + O \rightarrow NO + N$$
$$N + NO \rightarrow N_2(v \sim 3) + O$$
$$N + O_2 \rightarrow N + NO$$
$$N + \text{wall} \rightarrow NO$$
$$O + \text{wall} \rightarrow O_2$$

b) The rate coefficient for reaction $N_2(v > 12) + O \rightarrow NO + N$ is of the order of 10^{-11} $cm^3 \cdot s^{-1}$.

c) The wall losses of O and N atoms play an important role in controlling the populations of these species. By fitting the calculated values of these populations to the measured ones it has been shown that the wall loss probability depends on the relative population [O]/[N] and the gas temperature. Work is in progress to more precisely determine the kinetics of the interactions of N and O atoms on the wall.

d) The importance of associative ionization processes was shown for low O_2 percentages. Further investigations are necessary to study the kinetics of the excited levels such as $N_2(A)$, $N_2(a')$, $N_2(a'')$ involved in these processes.

To progress in the understanding of the kinetics more theoretical and experimental work is, of course, necessary. In particular, it should be interesting to study in more detail the dissociation processes of N_2 and to compare the measurements of the ionic composition to the model predictions.

Finally, it can be concluded that this model is a powerful tool to investigate N_2–O_2 discharges in a large range of experimental conditions.

Acknowledgment

The authors wish to thank A. R. de Souza, J. Amorim, G. Baravian, and M. J. G. Pinheiro for helpful discussions.

References

[1] V. Premachandran, "Etch rate enhancement of photoresist in nitrogen containing plasmas," *Appl. Phys. Lett.*, vol. 55, no. 24, pp. 2488–2490, 1989.

[2] A. Ricard, B. Berton, A. Bonnet, and M. P. Bacos, "Nitrogen and oxygen atoms production in N_2–O_2 microwave post-discharge," in *Proc. ESCAMPIG-XX*, Orléans, France, 1990, p. 195.

[3] B. Gordiets and A. Ricard, "Production of N, O and NO in N_2–O_2 flowing discharges," *Plasma Sources Sci. Technol.*, vol. 2, no. 3, pp. 158–163, 1993.

[4] A. R. de Souza, L. M. Malhmann, J. R. Muzart, and C. V. Speller, "Influence of nitrogen on the oxygen dissociation in a dc discharge," *J. Phys. D: Appl. Phys.*, vol. 26, pp. 2164–2167, 1993.

[5] J. Nahorny, D. Pagnon, M. Touzeau, and A. R. de Souza, "Study of the NO creation processes in a N_2–O_2 low pressure discharge," in *Proc. ICPIG-XXI*, Bochum, Germany, 1993, pp. 452–453.

[6] J. Nahorny, J. Amorim, G. Baravian, B. Gordiets, D. Pagnon, and M. Touzeau, "Determination of N_2 dissociation in a N_2–O_2 low pressure glow discharge," in *Proc. ISPC-XI*, Loughborough, England, 1993, pp. 603–608.

[7] J. Nahorny, D. Pagnon, M. Touzeau, M. Vialle, B. Gordiets, and C. M. Ferreira, "Experimental and theoretical investigation of a N_2–O_2 flowing glow discharge," submitted to *J. Phys. D: Appl. Phys.*, 1994.

[8] J. Loureiro and C. M. Ferreira, "Coupled electron energy and vibrational distribution functions in stationary N_2 discharges," *J. Phys. D: Appl. Phys.*, vol. 19, pp. 17–36, 1986.

[9] J. Loureiro and A. Ricard, "Electron and vibrational kinetics in an N_2–H_2 glow discharge with application to surface processes," *J. Phys. D: Appl. Phys.*, vol. 26, pp. 163–176, 1993.

[10] G. Gousset, C. M. Ferreira, M. Pinheiro, P. A. Sá, M. Touzeau, M. Vialle, and J. Loureiro, "Electron and heavy-particle kinetics in the low pressure oxygen positive column," *J. Phys. D: Appl. Phys.*, vol. 24, pp. 290–300, 1991.

[11] R. J. Henry, P. G. Burke, and A. L. Sinfailan, "Scattering of electrons by C, N, O, N^+, O^+ and O," *Phys. Rev. A*, vol. 178, pp. 218–225, 1969.

[12] D. Rapp and P. Englander-Golden, "Total cross-sections for ionization and attachment in gases by electron-impact. I) Positive ionization," *J. Chem. Phys.*, vol. 43, pp. 1464–1489, 1965.

[13] J. Loureiro, "Dissociation rate and $N(^4S)$ atom concentrations in a N_2 glow-discharge," *Chem. Phys.*, vol. 157, pp. 157–168, 1991.

[14] N. L. Alexandrov, A. M. Kouchakov, and E. E. Son, *Teplofiz. Vis. Temp.*, vol. 17, p. 4, 1979, in Russian.

[15] F. J. Mehr and M. A. Biondi, "Electron temperature dependence of recombination of O_2^+ and N_2^+ ions with electrons," *Phys. Rev.*, vol. 181, pp. 264–271, 1969.

[16] J. E. Frederick and D. W. Rusch, "On the chemistry of metastable atomic nitrogen in the F region deduced from simultaneous satellite measurements of the 5200 Å airglow and atmospheric composition," *J. Geophys. Res.*, vol. 82, pp. 3509–3517, 1977.

[17] E. C. Zipf, P. J. Espy, and C. F. Boyle, "The excitation and collisional desactivation of metastable $N(^2P)$ atoms in auroras," *J. Geophys. Res.*, vol. 85, pp. 687–694, 1980.

[18] F. L. Walls and G. H. Dunn, "Measurements of total cross-sections for electron recombination with NO^+ and O_2^+ using ion storage techniques," *J. Geophys. Res.*, vol. 79, pp. 1911–1915, 1974.

[19] D. G. Torr, M. R. Torr, H. C. Brinton, L. H. Brace, N. W. Spencer, A. E. Hedin, W. B. Hanson, J. H. Hoffman, A. O. Nier, J. C. G. Walker, and D. W. Rusch, "An experimental and theoretical study of the mean diurnal variation of O^+, NO^+, O_2^+ and N_2^+ ions in the mid-latitude F_1 layer of the ionosphere," *J. Geophys. Res.*, vol. 84, pp. 3360–3372, 1979.

[20] P. B. Hays, D. W. Rusch, R. G. Roble, and J. C. G. Walker, "The OI (6300 Å) airglow," *Rev. Geophys. Space Phys.*, vol. 16, pp. 225–232, 1978.

[21] E. C. Zipf, "Dissociative recombination of vibrationally excited O_2^+ ions," *J. Geophys. Res.*, vol. 85, pp. 4232–4236, 1980.

[22] M. R. Torr and D. G. Torr, "Associative ionization of $N(^2D)$ and O," *Planet. Space Sci.*, vol. 27, pp. 1233–1237, 1979.

[23] D. Kley, G. W. Lawrence, and E. J. Stone, "The yield of $N(^2D)$ atoms in the dissociative recombination of NO^+," *J. Chem. Phys.*, vol. 66, pp. 4157–4165, 1977.

[24] M. Fitaire, A. M. Pointu, D. Stathopoulos, and M. Vialle, "Measurement of N_4^+ recombination rate versus electron temperature in a proton beam created plasma," *J. Chem. Phys.*, vol. 81, pp. 1753–1758, 1984.

[25] L. S. Polak, P. A. Sergeev, and D. I. Slovetski, *Chimia Vis. Energii*, vol. 7, p. 387, 1973, in Russian.

[26] J. Keck and G. Carrier "Diffusion theory on non equilibrium dissociation and recombination," *J. Chem. Phys.*, vol. 43, pp. 2284–2298, 1965.

[27] B. F. Gordiets, A. I. Osipov, and L. A. Shelepin, *Kinetic Processes in Gases and Molecular Lasers*. New York: Gordon and Breach, 1986, translation from Russian.

[28] Yu. S. Akishev, A. V. Demianov, and I. V. Kochetov *Teplofis. Vis. Temp.*, vol. 20, pp. 818–827, 1982, in Russian.

[29] A. Lifshitz, "Correlation of vibrational deexcitation rate constant (k_{0-1}) of diatomic molecules," *J. Chem. Phys.*, vol. 61, pp. 2478–2479, 1974.

[30] R. McNeal, M. E. Whitson, Jr., and G. R. Cook, "Quenching of vibrationally excited N_2 by atomic oxygen," *Chem. Phys. Lett.*, vol. 16, p. 507, 1972.

[31] D. J. Eckstrom "Vibrational relaxation of shock-heated N_2 by atomic oxygen using the IR tracer method," *J. Chem. Phys.*, vol. 59, pp. 2787–2795, 1973.

[32] A. Lagana, E. Garcia, and L. Ciccarelli, "Desactivation of vibrationally excited nitrogen molecules by collision with nitrogen atoms," *J. Phys. Chem.*, vol. 91, p. 312, 1987.

[33] J. Frost and I. W. M. Smith, "Combining transition state theory with quasiclassical trajectory calculations: Application to the nitrogen exchange reaction $N + N_2(v)$," *Chem. Phys. Lett.*, vol. 140, no. 5, p. 499, 1987.

[34] B. Gordiets, *Geomagn. i Aeronomia*, vol. 17, pp. 871, 1977, in Russian.

[35] V. D. Rusanov and A. A. Fridman, *Physics of Chemically Active Plasma*. Moscow: Nauka, 1984, in Russian.

[36] L. S. Polak, M. Y. Goldeberg, and A. A. Levitskii, *Numerical Methods in Chemical Kinetics*. Moscow: Nauka, 1984, in Russian.

[37] I. K. Dmitrieva and V. A. Zenevich, *Khim. Fiz.*, vol. 3, p. 1075, 1984, in Russian.

[38] G. Black, R. Sharpless, and T. C. Slanger, "Measurements of vibrationally excited molecules by Raman scattering. I. The yield of vibrationally excited nitrogen in the reaction N + NO to N_2 + O," *J. Chem. Phys.*, vol. 58, pp. 4792–4797, 1973.

[39] L. G. Piper, "The excitation of $O(^1S)$ in the reaction between $N_2(A^3\Sigma_u^+)$ and $O(^3P)$," *J. Chem. Phys.*, vol. 77, no. 2, p. 2373–2377, 1982.

[40] A. R. de Souza and M. Touzeau, "Vibrational population of $N_2(C^3\Pi_u)$ in a nitrogen glow discharge," in *Proc. ICPIG*, Dusseldorf, Germany, 1983, vol. 16, no. 4, p. 355.

[41] A. R. de Souza, G. Gousset, M. Touzeau, and T. Khiet, "Note on the determination of the efficiency of the reaction $N_2(A^3\Sigma) + O(^3P) \rightarrow N_2 + O(^1S)$," *J. Phys. B: Atom. Mol. Phys.*, vol. 18, pp. L661–666, 1985.

[42] F. R. Gilmore, E. Bauer, and J. W. McGowan, "A review of atomic and molecular excitation mechanisms in nonequilibrium gases up to 20000 K," *J. Quant. Spectros. Radiat. Transfer*, vol. 9, p. 157, 1969.

[43] R. C. Flagan and J. P. Appleton, "Excitation mechanisms of the nitrogen first positive and first negative radiation at high temperature," *J. Chem. Phys.*, vol. 56, p. 1163, 1972.

[44] M. F. Golde and A. M. Moyle, "Study of the products of the reactions of $N_2(A^3\Sigma_u^+)$: The effect of vibrational energy in $N_2(A)$," *Chem. Phys. Lett.*, vol. 117, no. 4, p. 375, 1985.

[45] L. G. Piper, "The excitation of $N(^2P)$ by $N_2(A^3\Sigma_u^+, v' = 0{-}1)$," *J. Chem. Phys.*, vol. 90, no. 12, p. 7087, 1989.

[46] A. B. Calear and P. M. Wood, "Rates of energy transfer from $N_2(A^3\Sigma_u^+)$ to various molecules," *Trans. Faraday Soc.*, vol. 67, pp. 272–288, 1971.

[47] M. P. Iannuzzi, J. B. Jeffries, and F. Kaufman, "Product channels of the $N_2(A^3\Sigma_u^+) + O_2$ interaction," *Chem. Phys. Lett.*, vol. 87, no. 6, pp. 570–574, 1982.

[48] A. R. de Souza and M. Touzeau, "Quenching reactions of metastable $N_2(A^3\Sigma_u^+, v = 0, 1, 2)$ molecules by O_2," *Chem. Phys. Lett.*, vol. 121, no. 4, p. 423, 1985.

[49] M. E. Fraser and L. G. Piper, "Product branching ratios from $N_2(A^3\Sigma_u^+) + O_2$ interaction," *J. Phys. Chem.*, vol. 93, no. 3, pp. 1107–1111, 1989.

[50] W. G. Clark and D. W. Setser, "Energy transfer reactions of $N_2(A^3\Sigma_u^+.)5)$ Quenching by hydrogen halides, methyl halides and other molecules," *J. Phys. Chem.*, vol. 84, p. 2225, 1980.

[51] Cao De Zhao and D. W. Setser, "Energy transfer reactions of $N_2(A^3\Sigma_u^+)$ to SO and other diatomic and polyatomic molecules," *J. Phys. Chem.*, vol. 92, no. 5, pp. 1169–1178, 1988.

[52] J. W. Dreyer, D. Perner, and C. R. Roy, "Rate constants for the quenching of $N_2(A^3\Sigma_u^+, v = 08)$ by CO, CO_2, NH_3, NO and O_2," *J. Chem. Phys.*, vol. 61, p. 3164, 1974.

[53] G. N. Hays and H. J. Oskam, "Reaction rate constant for $2N_2(A^3\Sigma_u^+) \rightarrow N_2(C^3\Pi_u) + N_2(X\Sigma_g^+, v' > 0)$ (E)," *J. Chem. Phys.*, vol. 59, pp. 6088–6091, 1973.

[54] L. G. Piper, "State-to-state $N_2(A^3\Sigma_u^+)$ energy pooling reactions. II) The formation and quenching of $N_2(B^3\Pi_g, v' = 112)$," *J. Chem. Phys.*, vol. 88, no. 11, pp. 6911–6921, 1988.

[55] ——, "State-to-state $N_2(A^3\Sigma_u^+)$ energy pooling reactions. I) The formation of $N_2(C^3\Pi_u)$ and Herman infrared system," *J. Chem. Phys.*, vol. 88, no. 1, pp. 231–239, 1988.

[56] D. I. Slovetski, *Mechanisms of Chemical Reactions in the Nonequilibrium Plasma*. Moscow: Nauka, 1980, in Russian.

[57] N. A. Bogatov, M. S. Gitlin, S. V. Golubev, and S. V. Razin, in *Proc. XIX ICPIG*, Belgrade, Yugoslavia, 1989, p. 604.

[58] J. W. Dreyer and D. Perner, "The desactivation of $N_2(B^3\Pi_g, v = 02)$ and $N_2(a'^1\Sigma_u^-, v = 0)$ by nitrogen," *Chem. Phys. Lett.*, vol. 16, no. 1, p. 169, 1972.

[59] G. Black, T. C. Slanger, G. A. St. John, and B. A. Young, "Vacuum ultraviolet photolysis of N_2O, 4, deactivation of $N(^2D)$," *J. Chem. Phys.*, vol. 51, no. 1, p. 116, 1969.

[60] R. F. Heidner, D. G. Sutton, and S. N. Suchard, "Kinetic study of $N_2(B^3\Pi_g, v)$ quenching by laser-induced fluorescence," *Chem. Phys. Lett.*, vol. 37, no. 2, pp. 243, 1976.

[61] J. M. Calo and R. C. Axtmann, "Vibrational relaxation and electronic quenching of the $C^3\Pi_u$ state of nitrogen E," *J. Chem. Phys.*, vol. 54, pp. 1332, 1971.

[62] I. A. Kossyi, A. Yu. Kostinsky, A. A. Matveyev, and V. P. Silakov, "Kinetic scheme of the non-equilibrium discharge in nitrogen-oxygen mixtures," *Plasma Sources Sci. Technol.*, vol. 1, pp. 207–220, 1992.

[63] L. G. Piper, "Quenching rate coefficients for $N_2(a'^1\Sigma_u^-)$," *J. Chem. Phys.*, vol. 87, no. 3, pp. 1625–1629, 1987.

[64] A. B. Berdyshev, I. V. Kochetov, and A. P. Napartovich, *Fiz. Plazmy*, vol. 14, no. 6, p. 741, 1988, in Russian.

[65] Yu. B. Golubovsky and V. M. Telezhko, *Teplofis. Vis. Temp.*, vol. 22, no. 3, p. 428, 1984, in Russian.

[66] L. S. Polak, P. A. Sergeev, and D. I. Slovetski, *Teplofis. Vis. Temp.*, vol. 15, no. 1, p. 15, 1977, in Russian.

[67] D. E. Shemansky, "$A^3\Sigma_u^+$ molecules in the N_2 afterglow," *J. Chem. Phys.*, vol. 64, pp. 565–580, 1976.

[68] J. L. Delcroix, C. M. Ferreira, and A. Ricard, in *Principles of Laser Plasmas*, G. Bekefi, Ed. New York: Wiley, 1976, ch. 5.

[69] K. H. Becker, E. H. Fink, W. Groth, W. Jud, and D. Kley, "N_2 formation in the Lewis-Rayleigh afterglow," *Faraday Discuss. Chem. Soc.*, vol. 53, pp. 35–51, 1972.

[70] H. Partridge, S. R. Langhoff, C. W. Bauschlicher, and D. W. Schwenke, "Theoretical study of the $A'^5\Sigma_g^+$ and $C''^5\Pi_u$ states of N_2: Implications for the N_2 afterglow," *J. Chem. Phys.*, vol. 88, pp. 3174–3186, 1988.

[71] O. E. Krivonosova, S. A. Losev, V. P. Nalivaiko, Yu. K. Mukoseev, and O. P. Shatalov, *Plasma Chemistry* vol. 14, B. M. Smirnov, Ed. Moscow: Energizdat, 1987, in Russian, pp. 3–31.

[72] L. T. Cupitt, G. A. Takacs, and G. P. Glass, "Reaction of hydrogen atoms and oxygen $O_2(^1\Delta_g)$," *Int. J. Chem. Kinet.*, vol. 14, p. 487, 1982.

[73] A. O'Keefe, G. Mauclaire, D. Parent, and M. T. Bowers, "Product energy disposal in the reaction of $N^+(^3P)$ with $O_2(X^3\Sigma)$," *J. Chem. Phys.*, vol. 84, no. 1, pp. 215–219, 1986.

[74] A. P. Billington and P. Borell, "The low temperature quenching of singlet molecular oxygen $O_2(a^1\Delta_g)$," *J. Chem. Soc. Faraday Trans.*, vol. 82, pp. 963–970, 1986.

[75] R. Atkinson and K. H. Welge, "Temperature dependence of $O(^1S)$ desactivation by CO_2, O_2, N_2 and Ar*," *J. Chem. Phys.*, vol. 57, p. 3689, 1972.

[76] M. Yaron, A. von Engel, and P. H. Vidaud "The collisional quenching of $O_2^*(^1\Delta_g)$ by NO and CO_2," *Chem. Phys. Lett.*, vol. 37, no. 1, p. 159, 1976.

[77] B. Eliasson, "Electrical discharge in oxygen. Part 1: Basic data and rate coefficients.," Tech. Rep. KLR 83-40C, Brown Boveri, 1983.

[78] R. P. Wayne, in *Singlet O_2*, vol. 1, A. A. Frimer, Ed. Boca Raton, FL: CRC Press, 1985, p. 81.

[79] R. F. Heidner, C. E. Gardner, T. M. El-Sayed, G. I. Segal, and J. V. V. Kasper, "Temperature dependence of $O_2(^1\Delta) + O_2(^1\Delta)$ and $I(^2P_{1/2}) + O_2(^1\Delta)$ energy pooling," *J. Chem. Phys.*, vol. 74, p. 5618, 1981.

[80] T. G. Slanger and G. Black, "Interactions of $O_2(b^1\Sigma_g^+)$ with $O(^3P)$ and O_3," *J. Chem. Phys.*, vol. 70, pp. 3434–3438, 1979.

[81] P. M. Borrell, P. Borrell, K. R. Grant, and M. D. Pedley, "Rate constant for the energy-pooling and quenching reactions of singlet molecular oxygen at high temperatures," *J. Phys. Chem.*, vol. 86, pp. 700–703, 1982.

[82] K. Y. Choo and M. T. Leu, "Rate constants for the quenching of metastable $O_2(^1\Sigma_g^+)$ molecules," *Int. J. Chem. Kinet.*, vol. 17, pp. 1155–1167, 1985.

[83] R. J. O'Brien and G. H. Myers, "Direct flow measurements of $O_2(b^1\Sigma_g^+)$ quenching rates," *J. Chem. Phys.*, vol. 53, no. 10, p. 3832, 1970.

[84] K. H. Becker, W. Groth, and U. Schurath, "The quenching of metastable $O_2(^1\Delta_g)$ and $O_2(^1\Sigma_g^+)$ molecules," *Chem. Phys. Lett.*, vol. 8, pp. 259–262, 1971.

[85] M. J. Lopez-Gonzalez and R. Rodrigo, in *19th Annu. Europ. Meet. on Atmospheric Studies by Optical Methods*, Kiruna, Sweeden, 1992, p. 76.

[86] M. J. Lopez-Gonzalez, J. J. Lopez-Moreno, and R. Rodrigo, "Altitude profiles of the atmospheric system of O_2 and of the green line emission," *Planet Space Sci.*, vol. 40, pp. 783–795, 1992.

[87] J. E. Davenport, T. G. Slanger, and G. Black, "The quenching of $N(^2D)$ by $O(^3P)$," *J. Geophys. Res.*, vol. 81, pp. 12–16, 1976.

[88] D. Husain, S. K. Mitra, and A. N. Young, "Kinetic study of electronically excited nitrogen atoms $N(^2D, {}^2P)$ by attenuation of atomic resonance radiation in vacuum ultaviolet," *J. Chem. Soc. Faraday Trans.*, vol. 70, pp. 1721–1731, 1974.

[89] R. J. Donovan and D. Husain, "Recent advances in the chemistry of electronically excited atoms," *Chem. Rev.*, vol. 70, pp. 489–516, 1970.

[90] G. Black, R. L. Sharpless, T. G. Slanger, and D. C. Lorents, "Quantum yields for the production of $O(^1S)$, $N(^2D)$ and $N_2(A^3\Sigma_u^+)$ from the vacuum UV photolysis of N_2O," *J. Chem. Phys.*, vol. 62, pp. 4266–4273, 1975.

[91] D. Husain, "The reactivity of electronically excited species," *Ber. Bunsen-Ges. Phys. Chem.*, vol. 81, no. 2, pp. 168–177, 1977.

[92] B. Eliasson and U. Kogelschatz, "Basic data for modeling of electrical discharges in gases: Oxygen," Tech. Rep. KLR 86-11C, Brown Boveri, 1986.

[93] P. H. Wine and A. R. Ravishankara, "Kinetics of $O(^1D)$ interactions with the atmospheric gases N_2, N_2O, H_2O, H_2, CO_2 and O_3," *Chem. Phys. Lett.*, vol. 77, no. 1, pp. 103–109, 1981.

[94] T. G. Slanger and G. Black, "$O(^1S)$ quenching by $O(^3P)^*$," *J. Chem. Phys.*, vol. 64, pp. 3763–3766, 1976.

[95] W. Felder and R. A. Young, "Quenching of $O(^1S)$ by $O(^3P)^*$," *J. Chem. Phys.*, vol. 56, p. 6028, 1972.

[96] I. C. Slanger, B. G. Wood, and G. Black, "The temperature dependence of $O(^1S)$ quenching by O_2^*," *Chem. Phys. Lett.*, vol. 17, pp. 401–403, 1972.

[97] J. S. Levine, *The Photochemistry of Atmosphere*, 1st ed. New York: Academic, 1985, ch. 1.

[98] T. G. Slanger and G. Black "The product channels in quenching of $O(^1S)$ by $O_2(a^1\Delta_g)$," *J. Chem. Phys.*, vol. 75, pp. 2247–2251, 1981.

[99] R. D. Kenner and E. A. Ogryzlo, "A direct determination of the rate constant for quenching of atomic oxygen $O(^1S)$ by molecular oxygen $O_2(^1\Delta_g)$," *J. Photochem.*, vol. 18, no. 4, p. 379, 1982.

[100] G. London, R. Gilpin, H. I. Schiff, and K. H. Welge, "Collisional desactivation of $O(^1S)$ by O_3 at room temperature," *J. Chem. Phys.*, vol. 54, p. 4512, 1971.

[101] S. V. Filseth, F. Stuhl, and K. H. Welge, "Collisional desactivation of $O(^1S)$," *J. Chem. Phys.*, vol. 57, p. 4064, 1972.

[102] S. W. Benson, D. M. Golden, R. Shaw, R. W. Woolfolk, and R. W. Lawrence "Estimation of rate constant as a function of temperature for reactions $X + YZ \rightleftharpoons XY + Z, X + Y + M \rightleftharpoons XY + M$ and $X + YZ + M \rightleftharpoons XYZ + M$, where X, Y and Z are atoms, hydrogen, nitrogen, oxygen," in *Int. J. Chem. Kinet. Symp.*, 1975, no. 1, pp. 399–440.

[103] D. L. Baulch, D. D. Drysdale, and D. C. Horne, Eds., *Homogeneous Gas Phase Reactions of the H_2, N_2, O_2 Systems*, no. 2. London: Butterworths, 1973.

[104] L. J. Stief, W. A. Payne, J. H. Lee, and J. V. Michael "The reaction $N(^4S) + O_3$: An upper limit for the rate constant at 298 K," *J. Chem. Phys.*, vol. 70, no. 11, pp. 5241–5243, 1979.

[105] D. L. Baulch, D. D. Drysdale, J. Duxbary, and S. L. Grant, Eds., *Homogeneous Gas Phase Reactions of the O-O Systems, CO, O, H Systems and Sulphur-Containing Species*, no. 3. London: Butterworths, 1976.

[106] L. A. Viehland and E. A. Mason "Statistical mechanical theory of gaseous ion-molecule reactions in an electrostatic field," *J. Chem. Phys.*, vol. 66, pp. 422–434, 1977.

[107] J. P. St-Maurice and D. G. Torr "Non thermal rate coefficients in the ionosphere: The reactions of O^+ with N_2, O_2 and NO," *J. Geophys. Res.*, vol. 83, pp. 969–977, 1978.

[108] J. Zinn, C. D. Sutherland, S. N. Stone, and L. M. Duncan, "Ionospheric effects of rocket exhaust products—HEAO-C Skylab," *J. Atmos. Terr. Phys.*, vol. 44, no. 12, pp. 1143–1171, 1982.

[109] M. J. McEwan and L. F. Phillips, *Chemistry of the Atmosphere*, vol. 1, 1st ed. Edward Arnold, 1975, ch. 1.

[110] E. W. McDaniel, V. Cermak, A. Dalgarme, E. G. Ferguson, and L. Friedman, *Ion-Molecule Reactions*, 1st ed. New York: Wiley, 1970, ch. 1.

[111] S. I. Kozlov, V. A. Vlaskov, and N. V. Smirnova, *Sov. Space. Res.*, vol. 26, no. 5, p. 738, 1988, in Russian.

[112] M. H. Bortner and T. Baurer, *Defense Nuclear Agency Reaction Rate Handbook*, General Electric TEMPO, 1978.

[113] F. C. Fehsenfeld and E. E. Ferguson, "Recent laboratory measurements of D and E region ion-neutral reactions," *Radio Sci.*, vol. 7, pp. 113–115, 1972.

[114] D. L. Albritton, "Atom. nucl. data tables," Tech. Rep. N1, 1979.

[115] F. E. Niles, "Survey of two-body and three-body reaction rate coefficients for the ionized stratosphere and mesosphere," Tech. Rep. 1702, U. S. Army Aberdeen Proving Grounds, MD, 1974.

[116] R. Haug F. Bastien, and M. Lécuiller, "Simulation sur ordinateur de l'évolution temporelle des ions négatifs de l'air. Application au cas de la décharge couronne négative," *J. Chimie Phys.*, vol. 72, no. 1, pp. 105–112, 1975.

[117] N. L. Alexandrov, *Zh. Techn. Fis.*, vol. 48, no. 7, pp. 1428–1431, 1978, in Russian.

[118] H. Sabadil, P. Bachmann, and Kastelewicz, "Reaction kinetics of ozone generation in the oxygen glow discharge," *Beitr. Plasma Phys.*, vol. 20, no. 4, pp. 283–295, 1980.

[119] T. Grigorieva, A. Levitsky, S. Macheret, L. S. Polak, V. Rusanov, and A. Fridman, *Chimia Vis. Energii*, vol. 18, no. 4, p. 336, 1984, in Russian.

[120] C. M. Ferreira, G. Gousset, and M. Touzeau "Quasi-neutral theory of positive columns in electronegative gases," *J. Phys. D: Appl. Phys.*, vol. 21, pp. 1403–1413, 1988.
[121] S. C. Brown, *Basic Data of Plasma Physics*, 2nd ed. Boston: MIT Press, 1967.
[122] M. Touzeau, M. Vialle, A. Zellagui, G. Gousset, M. Lefebvre, and M. Pealat, "Spectroscopic temperature measurements in oxygen discharge," *J. Phys. D: Appl. Phys.*, vol. 24, pp. 41–47, 1991.
[123] J. Amorim, G. Baravian, J. Jolly, and M. Touzeau, "Two-photon laser induced fluorescence and amplified spontaneous emission atom concentration measurements in O_2 and H_2 discharges," *J. Appl. Phys.*, vol. 76, 1994, to be published.
[124] D. Pagnon, J. Amorim, J. Nahorny, M. Touzeau, and M. Vialle, "Concentration of atoms in O_2 glow discharges by actinometry. Comparison with absolute measurements by VUV resonant absorption," in *Proc. ICPIG-XX*, Pisa, Italy, 1991, pp. 1445–1446.
[125] W. L. Wiese, M. W. Smith, and B. M. Miles, *Atomic Transitions Probabilities*, vol. 2. Washington, DC: Nat. Bur. Stand., 1969.
[126] A. Belikov, private communication, 1992.
[127] J. K. Ballou, C. C. Lin, and F. E. Fajen "Electron-impact excitation of the argon atom," *Phys. Rev. A*, vol. 8, p. 1797, 1973.
[128] P. J. Dagdigian, B. E. Forch, and A. W. Miziolek, "Collisional transfert between and quenching of the $3p^3P$ and ^5P states of the oxygen atoms," *Chem. Phys. Lett.*, vol. 148, p. 299, 1988.
[129] J. Bittner, K. Kohse-Höinghaus, U. Meier, and T. Just "Quenching of two-photon-excited $H(3s, 3d)$ and $O(3p^3P_{2,1,0})$ atoms by rare gases and small molecules," *Chem. Phys. Lett.*, vol. 143, p. 571, 1988.
[130] D. J. Bamford, L. E. Jusinski, and W. K. Bischel, "Absolute two-photons absorption and three-photon ionization cross-sections for atomic oxygen," *Phys. Rev. A*, vol. 34, p. 185, 1986.
[131] W. K. Bischel, B. E. Perry, and D. R. Crosley, "Two-photon laser induced fluorescence in oxygen and nitrogen atoms," *Chem. Phys. Lett.*, vol. 82, p. 85, 1981.
[132] P. S. Julienne and J. Davis, "Cascade and radiation trapping effects on atmospheric atomic oxygen emission excited by electron impact," *J. Geophys. Res.*, vol. 81, p. 1397, 1976.
[133] E. E. Gulcicek, J. P. Doering, and S. O. Vaughan, "Absolute differential and integral electron excitation cross-sections for atomic oxygen $^3P \rightarrow {}^3P$ and $^3P \rightarrow {}^5P$ transitions from 13.87 to 100 eV," *J. Geophys. Res.*, vol. 93, p. 5885, 1988.
[134] M. B. Schulman, F. A. Sharpton, S. Shung, C. C. Lin, and L. W. Anderson, "Emission from oxygen atoms produced by electron-impact dissociative excitation of oxygen molecules," *Phys. Rev. A*, vol. 32, p. 2100, 1985.
[135] H. Brunet and J. Rocca-Serra, "Model for a glow discharge in flowing nitrogen," *J. Appl. Phys.*, vol. 57, no. 5, pp. 1574–1581, 1985.
[136] Yu. B. Golubovsky and V. M. Telezhko, "Measurements of the vibrational temperature of the ground state of N_2 according to the emission of the N_2^+ molecular ion," *J. Appl. Spectrosk.* (USSR), vol. 39, pp. 1429–1431, 1983.

Boris F. Gordiets was born in Chelabinsk, Russia, on September 23, 1941. He graduated from the Moscow Physical–Technical Institute (in Dolgoprudniy) as a engineer-physicist and has received the degree of Candidate of Science in 1968 and the degree of Doctor of Science in 1982.

Since 1968 he has been with the P.N. Lebedev Physical Institute of the Russian Academy of Sciences as a Leading Scientist (since 1986) and chief of scientific group. He is at present an Invited Professor at the Instituto Superior Tecnico and Researcher at the Centro de Electrodinamica, Universidade Técnica de Lisboa, Lisbon, Portugal. His scientific interest is theoretical investigations and modeling of kinetic processes in molecular physics, physics of gas lasers, atmospheric and ionospheric physics and chemistry, and physics of low-temperature plasma.

Carlos M. Ferreira was born in Lisbon, Portugal, on June 27, 1948. He graduated in electrical engineering from the Instituto Superior Técnico (IST), Lisbon Technical University, in 1971, and received the degree of Docteurés-Sciences Physiques from the University of Paris-XI, Orsay, in 1976.

Since 1979 he has been a Full Professor at the Physics Department of IST, and served as Head of Department during 1984–1987 and 1992–1994. He heads a research group on nonequilibrium processes in gas discharges at the Centro de Electrodinamica of IST.

Dr. Ferreira has been the Secretary-General of the Portuguese Physical Society since 1990, a member of the EPS Council since 1989, and has served on the EPS Executive Committee since 1992.

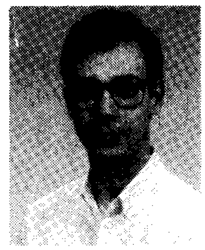

Vasco L. Guerra was born in Torres Vedras, Portugal, on December 12, 1968. He graduated in physical engineering from the Instituto Superior Técnico (IST), Lisbon Technical University, in 1991, and received the M.Sc. degree in plasma physics from IST in 1994. He is now working at IST towards the Ph.D. degree.

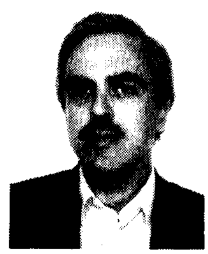

Jorge M. A. H. Loureiro was born in Lisbon, Portugal, in 1951. He graduated in electrical engineering from the Instituto Superior Técnico (IST) (Lisbon Technical University), in 1976, and received the Ph.D. degree in physics from the same University in 1987.

He has been an Assistant Professor at the Physics Departament of IST since 1976, and an Associate Professor since 1993. His work is concentrated on the Boltzmann and vibrational kinetics in dc and HF discharges in pure molecular gases and their mixtures.

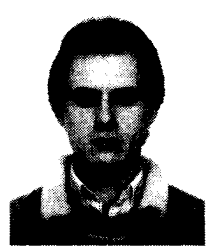

Jacimar Nahorny received the master degree at the University Federal of Santa Catarina (Brazil) in 1990. He is now a fellow of the 'Conselho National de Pesquisa' working toward the degree of 'Docteur es Sciences Physique' at the 'Laboratoire de Physique des Gaz et des Plasmas,' University of Paris-Sud.

His present research interests concern the kinetics of molecular discharges.

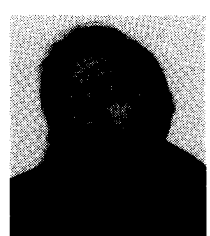

Daniel Pagnon graduated in physics and metrology from the 'Conservatoire des Arts et Métiers' in 1975. He received the degree of 'Docteur es Sciences Physiques' from the University of Paris-Sud in 1992.

At present he is 'Ingénieur de Recherches' at the 'Centre National de la Recherche Scientifique.' His research activities include the study and the applications of discharges.

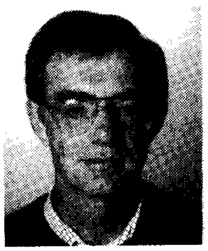

Michel Touzeau received the degree of 'Docteur es Sciences Physiques' from the University of Paris, Orsay, in 1977.

At present he is 'Directeur de Recherches' at the 'Centre National de la Recherche Scientifique.' His current scientific activities at the 'Laboratoire de Physique des Gaz et des Plasmas' concern the kinetics of nonequilibrium plasmas and the application of discharges to surface treatment and plasma chemistry.

Marinette Vialle received the degree of 'Docteur es Sciences Physiques' from the University of Paris-Sud in 1983 for studies on nuclear induced plasmas.

She joined the 'Laboratoire de Physique des Gaz et des Plasmas' at Orsay in 1976. Since 1989 she has been Professor at the 'Conservatoire des Arts et Métiers' in Paris. Her current research activities concern the study of discharges in molecular gases and their applications.